SENSORLESS WAVE BASED CONTROL

By

ISLAM S. M. KHALIL

Submitted to the Graduate School of Engineering and Natural Science
in partial fulfillment of
the requirements for the degree of
Master of Science

Sabanci University
Spring, 2009

SENSORLESS WAVE BASED CONTROL

ISLAM S. M. Khalil

APPROVED BY:

Prof. Dr. Asif Sabanovic (Thesis Advisor)
_____

....

Assoc. Prof. Dr. Mahmut AKSIT
_____

....

Assist. Prof. Dr. Kemalettin ERBATUR
_____

....

Assit. Prof. Dr. Hakan ERDOGAN
_____

....

Assist. Prof. Dr. Ali KOSAR
_____

....

DATE OF APPROVAL: ....

To my Mom Samia who gave me the means.

VITA

Islam Shoukry Mohammed Khalil

Candidate for the Degree of

Master of Science

Thesis: SENSORLESS WAVE BASED CONTROL

Major Field: Mechatronics Engineering

Biographical:

Islam shoukry mohammed was Born in Cairo, Egypt. He received his B.S. degree in Mechanical engineering from Helwan University, Cairo, Egypt in 2006. His research interests includes modeling and control of dynamical systems, motion and vibration control, nonlinear control, stress analysis, fracture mechanics, mechanical system design and Mechatronics.

The following were published out of this thesis:

1. Islam S. M. Khalil and Asif Sabanovic,"Sensorless Wave Based Control of Flexible Structures Using Actuator as a Single Platform For Estimation and Control", In *International Review of Automatic Control (IREACO)* Janauary, 2009, Vol 2, N 1, PP 83-89.

2. Islam S. M. Khalil, E. D. Kunt and Asif Sabanovic, "Sensorless Wave Based Control of Flexible Systems", *Tok'08*, Automatic Control Conference, Istanbul, October 15, Vol 2, PP 725-730. (Best Student Paper Award).

3. Islam S. M. Khalil, E. D. Kunt and Asif Sabanovic, "A Novel Algorithm for Sensorless Motion Control, parameters Identification and position Estimation", In *Turkish Journal Of Electrical Engineering And Computer Science*, 2009. (to appear in 2009 issue)

4. Islam S. M. Khalil, E. D. Kunt and Asif Sabanovic, "Sensorless Wave Based Parameter Detection and Position Estimation", *IEEE-International Conference on Intelligent Robots and Systems-IROS* 2009, (In review).

5. Islam S. M. Khalil, E. D. Kunt and Asif Sabanovic, "Estimation Based PID Controller-Sensorless Wave Based Technique", *IFAC-International Conference on Intelligent Control Systems and Signal Processing-ICONS* 2009. (to appear in IFAC proceeding 21-23 Sept. 2009)

6. Islam S. M. Khalil, A. Teoman Naskali and Asif Sabanovic, "On Fraction Order Modeling and Control of Dynamical Systems", *IFAC-International Conference on Intelligent Control Systems and Signal Processing-ICONS* 2009. (to appear in IFAC proceeding 21-23 Sept. 2009)

7. Islam S. M. Khalil and Asif Sabanovic, "Sensorless Torque Estimation In Multidegree-of-freedom Flexible Systems", *IEEE-International Symposium on Computational Intelligence in Robotics and Automation-CIRA* 2009, (In review).

8. Islam S. M. Khalil, E. D. Kunt and Asif Sabanovic, "Sensorless Motion Control of Multidegree-of-freedom Flexible systems", *IEEE-Industrial Electronics Society-IECON* 2009, (In Review).

ACKNOWLEDGMENTS

SENSORLESS WAVE BASED CONTROL

Islam Shoukry Mohammed Khalil

Mechatronics Engineering, MS thesis, 2009

Thesis Supervision: Prof. Dr. Asif Sabanovic

Keywords: Mechanical waves, sensorless motion and vibration control, position estimation, force estimation, estimation based controllers

Abstract

Mechanical waves naturally propagate through dynamical systems that are subjected to initial excitation. These mechanical waves carry enough information about the dynamical system including its dynamics and parameters, in addition to the externally applied forces or torques due to the system's interaction with the environment. In other words, mechanical waves carry all the dynamical system's information in a coupled fashion. This thesis proposes an estimation algorithm that enables estimating flexible systems' dynamics, parameters, externally applied forces and disturbances. The proposed algorithm is implemented on a lumped system with an actuator located at one of its boundaries, that is used as a single platform for measurements where actuator's current and velocity are measured and used to estimate the reflected mechanical waves. Only these two measurements from the actuator are required to accomplish the motion and vibration control, keeping the dynamical system free from any attached sensors by considering the reflected mechanical waves as a natural feedback from the system. In this thesis the notion of position estimation is proposed including both rigid and flexible motion estimation, where the position of each lumped mass is estimated and experimentally compared with the actual measurements. This in turn implies the possibility of using these position estimates as a virtual feedback to the controllers instead of using the actual sensor's feedback. System's global behavior can be investigated by monitoring lumped system dynamics, to guarantee the accomplishment of motion control task and the minimization of system's residual vibrations. Since the dynamics of the system can be obtained, the externally applied forces or torques can be estimated. The experimental results show the validity of the proposed algorithm and the possibility of using two actuator parameters in order to estimate the uniform system parameters, rigid system's position, flexible system's lumped mass positions and external disturbances due to system's interaction with the environment.

TABLE OF CONTENTS

LIST OF TABLES

CHAPTER 1

Introduction

Interest in flexible robots and structures is ever-growing due to the lighter loads they provide, higher acceleration that can be achieved, low power consumption, low material and manufacturing costs, better load to weight ratio, and less powerful actuator requirement compared to rigid robots. On the other hand, there arise some difficulties related with structural flexibility.

Firstly, dynamics and kinematics analysis of flexible manipulators and robots are very difficult since exact modeling of vibration modes is nearly impossible and the kinematics map is also inaccurate. In addition, the controller design is not easy because of the uncontrollable nature of system dynamic states, that comes from insufficient number of control inputs. Moreover, non-collocated sensing gives the system non-minimum phase property which limits the control performance. Furthermore, flexible structures suffer from the ever-lasting vibrations due even slightest manoeuvres, that add more complexity to the controller that has to take care of extra secondary tasks such as vibration suppression.

Besides, sensors have to possess sufficient specifications such as fatigue resistance to withstand the fluctuating stresses imparted by the flexible structure. Furthermore, extra sensors have to be used if both motion and vibration control are considered since feedback signal is required from the point of interest to be controlled along with the measurements of the other points to guarantee that system is controlled and residual vibrations are suppressed. The number of sensors required for a certain control process can be reduced by proper observers, but additional measurements

1

have to be taken from the system providing that the system is guaranteed to be observable. In other words, observers help to cut down the number of sensors attached to the dynamical system. Surprisingly enough that all these sensors can be avoided and dynamical system can be free from any attached sensors if the mechanical waves were measured or estimated and analyzed to extract the necessary information for the control process. Simply, system parameters and position feedback are required for a motion and vibration control, while force control requires the extraction of the force information from the mechanical waves.

The questions that arise are whether these mechanical waves include all of this information, whether they can be estimated or measured from the actuator side, and finally whether the system's parameters, dynamics and disturbance can be decoupled and each piece of information can be extracted out of the reflected mechanical waves.

Firstly, a mathematical expression of the reflected mechanical wave has to be explored and obtained from the set of equations of motion that describe the system's dynamics. Secondly, the nature of the mechanical waves' propagation have to be studied and analyzed to know whether they can be detected from the actuator side. And above all, the capability of decoupling each piece of information out of the reflected waves requires full understanding of the dynamical system behavior through the entire system's frequency range.

Modal analysis, frequency response analysis and input shaping represent the core of the sensorless estimation algorithm presented in this thesis. Two measurements are taken from the actuator and used as the input for a chain of observers to estimate the system's uniform parameters, rigid body position, flexible lumped positions and external disturbances. Using all of these estimates, sensorless motion and vibration controllers can be constructed without taking any measurement from the flexible system.

1.1 Definition and Overview

Mechanical wave is a local oscillation of the material, where only the energy propagates while the oscillating material does not move far from its initial equilibrium position. This wave is created in a certain media when energy is added by any arbitrary input that forces this wave to propagate between the finite length media's boundaries.

These mechanical waves can be considered as a propagating force, torque, displacement, velocity or acceleration waves. They carry some information about the media through which they propagate. In the next chapters, we will show that waves reconstruct each other at system's boundaries at which an actuator exists to launch the initial input excitation energy.

Historically, the problem of the vibrating string and the associated propagating waves was investigated by D'Alembert, Euler, Bernoulli and Lagrange, and the one dimensional wave equation was solved by D'Alembert. Waves were studied in different fields and for large variety of applications but rarely used in the field of dynamical system control until 1998, when O'Connar used actuator to launch and absorb mechanical waves in the system to achieve precise motion control by taking one measurement from the system in the absence of disturbance and any applied external forces O'Connar [1].

Energy and momentum enter and leave the flexible system at the actuator/system interface. Motion of the actuator should get the energy and momentum into and then out of the system in the right way to ensure that the entire system comes to rest at the target, which is the central idea of the wave based control O'Connar [2].

Wave transfer function was proposed in O'Connar [3] that maps the position of each system's lumped mass with it's neighbor. This transfer function suggests that motion of each lumped mass is given exactly by the superposition of a rightward and leftward motion of the lumped mass, or the launch and absorb waves at actua-

tor/system interface.

The same interpretation can be obtained by solving the one dimensional wave equation where the solution represents a wave moving to the left added to another one moving with the same velocity in the opposite direction. This result was used to construct a motion and vibration control law for lumped flexible robots using single measurement from the flexible system besides the actuator's measurements O'Connar [4].

Mechanical waves were used to analyze and control gantry cranes in O'Connar [5]. Simply, the control strategy depends on moving the trolley short away of the target and allowing the load to swing to the target. At this point the controller moves the trolley to the target position. More precisely, the controlled trolley launches and absorbs waves that travel to and from the load by separating these waves into outgoing and returning waves, each treated differently by the motion of the trolley O'Connar [6].

A comparison between wave based control and other schemes for controlling flexible structures such as linear quadratic regulator, Bang-Bang control and input shaping was presented in Mckeown [7]. The first scheme requires the knowledge of all the system's states or their estimates, while the other approaches require the exact and complete model as they are entirely open loop. On the other hand, the wave based approach can be extended to n degree-of-freedom using only single measurement from the first lumped mass. Nonlinear behavior of wave based control was investigated in O'Connar [8].

Despite of the promising results obtained by the researchers in this field, the success and robustness of the control process is not guaranteed unless certain assumptions are made, such as neglecting the external disturbances due to the interaction with the environment. Furthermore, a measurement has to be taken from the system despite the natural feedback provided by the reflected waves on the actuator. Indeed, taking

single measurement from the dynamical system and accomplishing the motion and vibration control task successfully is advantageous, but it also indicates that system's natural feedback is not fully utilized.

The aim of this thesis is to accomplish motion, vibration and force control without taking any measurement from the dynamical system. Therefore, the mechanical waves are treated differently, and defined in a way that enables to extract as much information as possible out of the reflected mechanical wave if not all the information.

Surprisingly enough that in the last few decades reflected mechanical waves and many other terms were considered as disturbance, and observers were designed to estimate such disturbances from the actuator using its parameters Hirotaka [9]. On one hand, rejecting the disturbance that includes the reflected mechanical wave and many other terms makes the control system robust by turning the control system into acceleration control if certain assumptions are made. On the other hand, the total disturbance contains several terms such as columb friction, variation of self-inertial torque, torque ripples, externally applied forces and the reflected mechanical waves or the reflected load that contains enough information about the dynamical system. Therefore, the reflected mechanical wave has to be extracted out of the total disturbance.

Disturbance observer was designed in Ohnishi [10]-[11] by measuring the actuator's current and velocity, then disturbance was estimated through a low pass filter. The disturbance observer was supported by some velocity measurement methods to avoid the direct differentiation of the optical encoder signal Toshiaki [12]. As the reflected mechanical wave is of our concern, the disturbance observer has to be modified in order to decouple this reflected wave out of the total disturbance. Murakami [13]-[14] showed that the reflected torque can be decoupled out of the total estimated disturbance by performing a parameters identification process. Performance of the disturbance observer was investigated in Seiichiro [15]-[10]. The frequency range

5

at which the observer is properly performing can be determined by the observer's sensitivity function Erwin [16].

Not only sensorless motion control is considered in this thesis but also sensorless vibration control and monitoring. Among the vibration control techniques Point-to-point motion/vibration control is a suitable control scheme for lumped flexible robots Miu [17]-[18] where the input waveform is selected such that at the end of the travel, there will be zero potential and zero kinetic energy stored in the system's elastic elements Bhat [19]. Control input was filtered using a low-pass filter or a notch filter in Sugiyama [20], in order to take away any energy at the resonant frequencies of the system such that system's flexible modes will not be excited. Similar results were obtained in Aspinwall [21]- Meckl [22] as the control input was Fourier synthesized to reduce excitation of the system's flexible modes. In this thesis the control input is Fourier synthesized or filtered in order not to excite certain modes of the flexible system, this allows minimizing the number of coordinates used to describe the system's motion. Therefore, certain system information can be estimated from specific system's frequency range.

1.2   Contribution of the Thesis

Strictly speaking, the word 'sensorless' is not correct, since one must measure or sense some variables to obtain some information as the basis of estimating the unknown variables and parameters. The flexible dynamical system is kept free from any measurement or any attached sensors excluding the actuator. Therefore, the word 'sensorless' in this context indicates that flexible part of the system is free from measurements. Only two variables are required from the actuator's side. In other words, actuator can be used as a single platform for measurement, estimation and control without taking any measurement from the flexible system.

This thesis investigates the following topics:

- Sensorless system parameter estimation

  System parameters such as stiffness of joints and damping coefficients are of great importance for the success of the control system design. Therefore, as a first step toward achieving sensorless wave-based control task, these parameters have to be estimated from the reflected mechanical wave. Fig.1.1. illustrates the parameter estimation process, where only actuator parameters are required. The details are explained in Chapter 3.

- Sensorless position estimation

  In this thesis the concept of motion estimation is presented. The motion of flexible dynamical systems can be rigid or flexible. Both of these motions are estimated using a chain of observers and an off-line experiment. This in turn implies that system's dynamics can be available as soon as these positions are successfully estimated. Fig.1.2. illustrates the position observer that is designed in Chapter 3.

- Sensorless motion and vibration control

  Estimating the system's flexible motion makes it possible to feedback these position estimates to the controller instead of the actual measurements taken by some attached sensors. The proposed position estimation algorithm presented in this thesis makes it possible to obtain the position estimates of all system's
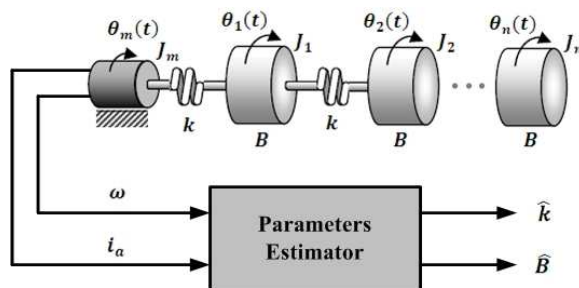
Figure 1.1: Illustration of system parameter estimation
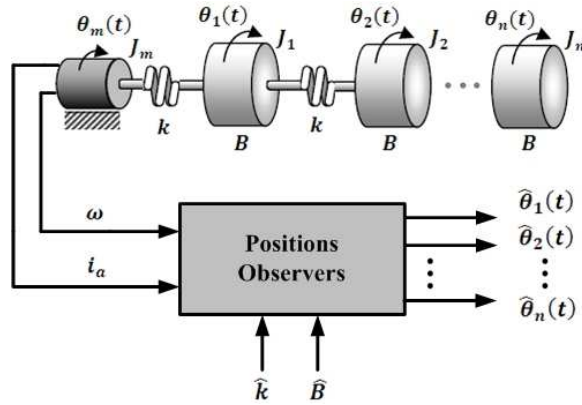
Figure 1.2: Illustration of system's position estimation

lumped masses. Therefore, controlling any mass or point of interest in the system is much easier and advantageous using this method, because of the simplicity of feeding these estimates back to the controller as they are all available. On the other hand, using the actual measurement as a feedback necessitates using multiple sensors or physically changing the sensor's location according to the mass of interest. Fig.1.3 illustrates the idea of the sensorless motion control, where the position estimates are used as feedback instead of the actual measurement.
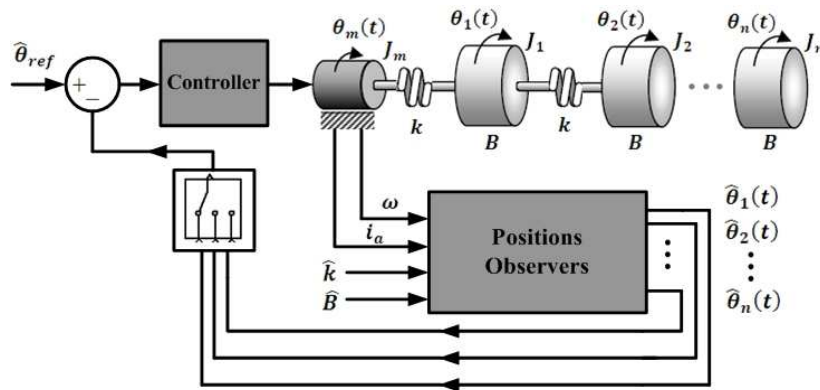
Figure 1.3: Illustration of the sensorless motion control

- Sensorless force estimation

Externally applied forces or disturbances on the system have to be considered

8

when the dynamical system has to perform a control task that requires interaction with the environment. And since the system's dynamics can be estimated, external forces also can be decoupled out of the reflected mechanical waves. Fig.1.4. illustrates the estimation process of an externally applied torque on the last inertial mass. The process starts with two measurements from the actuator and ends up with estimates of the system parameters, dynamics and external applied forces.
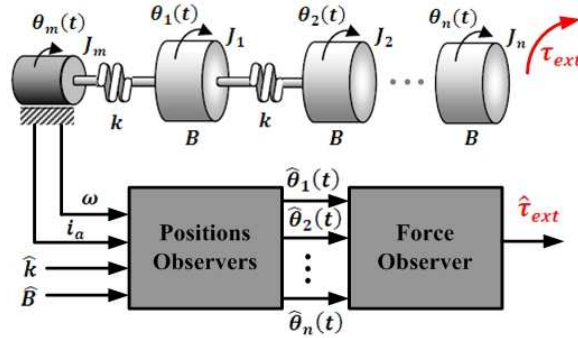
Figure 1.4: Illustration of the sensorless force estimation

1.3 Organization of the Thesis

This thesis is organized as follows. In Chapter 2, modal analysis and frequency response analysis of a flexible lumped system are studied. Reflected mechanical waves are investigated and shown to contain enough information about the system, moreover proved to be accessible from the actuator side. In Chapter 3, reflected mechanical waves are estimated using available actuator measurements. Uniform system parameters are estimated, and rigid body motion observer is designed. Then a chain of observers is designed to estimate the system's flexible motions. These estimates are used to accomplish sensorless motion and vibration control for flexible systems. In addition, external forces or torques due to system's interactions with the environment are estimated. Experimental results and the entire sensorless estimation algorithm are

9

included in Chapter 4. Final remarks, conclusions and recommendations for future work are included in Chapter 5.

CHAPTER 2

Modal Analysis of Lumped Flexible Systems

In this chapter, a lumped flexible system is modeled, mechanical waves are mathematically defined and shown to contain all system information including its parameters, dynamics and external disturbances. Then solution of the wave equation is compared with a transfer function interpretation to show that mechanical waves are accessible from the actuator side. Frequency response and modal analysis are investigated and used as the core of the estimation algorithm presented in Chapter 3 since the input forcing function is shaped, pre-filtered or synthesized according to these analyses.

2.1 Mechanical Waves in Flexible Systems

2.1.1 Modeling of lumped flexible systems

A lumped mass spring system is quite suitable for the purpose of this thesis as its parameters including the joint stiffness and the damping coefficients are to be estimated, and its dynamics including the positions, velocities, accelerations of each lumped mass, and finally the external disturbances are to be observed from the actu-
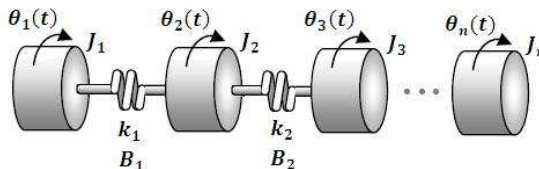
Figure 2.1: Lumped flexible inertial system

ator side. The matrix equation of motion for an n degree-of-freedom flexible system that is shown in Fig.2.1 is

$$[J][\ddot{\Theta}] + [B][\dot{\Theta}] + [K][\Theta] = \tau \tag{2.1}$$

J, B and K are the inertia, damping and stiffness matrices, Θ and τ are the system's generalized coordinate and external torque vectors.

$$\Theta = [\theta_1 \ \theta_2 \ \theta_3 \ \ldots \ \theta_n]'$$

$$\tau = [\tau_1 \ \tau_2 \ \tau_3 \ \ldots \ \tau_n]'$$

$$J = \begin{bmatrix} J_1 & 0 & 0 \\ 0 & \ddots & 0 \\ 0 & 0 & J_n \end{bmatrix}, B = \begin{bmatrix} B_1 & -B_1 & 0 \\ -B_1 & \ddots & -B_{n-1} \\ 0 & -B_{n-1} & B_{n-1} \end{bmatrix}, K = \begin{bmatrix} k_1 & -k_1 & 0 \\ -k_1 & \ddots & -k_{n-1} \\ 0 & -k_{n-1} & k_{n-1} \end{bmatrix}$$

Taking Laplace transform of Eq.2.1 and arranging the terms in the linear system form, assuming that $n = 3$

$$\mathbf{A} \ \Theta = \tau \tag{2.2}$$

where,

$$\mathbf{A} = \begin{bmatrix} J_1 s^2 + B_1 s + k_1 & -B_1 s - k_1 & 0 \\ -B_1 s - k_1 & J_2 s^2 + (B_1 + B_2)s + k_1 + k_2 & -B_1 s - k_1 \\ 0 & -B_1 s - k_1 & J_3 s^2 + B_2 s + k_2 \end{bmatrix}$$

Solving the determinant of $\mathbf{A}$ assuming equal masses, damping coefficients and spring constants, we obtain the following characteristic equation

$$m^3 s^6 + 4m^2 \beta s^5 + (4m^2 k + 3m\beta^2)s^4 + 6m\beta k s^3 + 3mk^2 s^2 = 0 \tag{2.3}$$

Solving for the roots of the characteristic equation Eq.2.3, assuming zero damping coefficient we get

$$s_{1,2} = 0$$
$$s_{3,4} = \pm j\sqrt{\frac{k}{m}}$$
$$s_{5,6} = \pm j\sqrt{\frac{3k}{m}}$$

These are the poles of the system which depend on the mass distribution, stiffness and damping through the system, They all fall on the imaginary axis since the damping coefficients are all zeros. Moreover, they do not depend on the position of force application and the positions from which measurements are taken.

Unlike the poles, zeros of the system depend on the SISO system. In other words, they depend on the position where the force is applied and the measurements are taken, this in turn implies that we have nine sets of zeros corresponding to nine different input output configurations. The system's poles and zeros are shown in Fig.2.2 and Fig.2.3.

As the position of measurement is moved along the flexible structure, the zeros immigrate toward or far away from the origin of the complex plane. When a zero coincides with a pole as shown in Fig.2.3, we lose the observability due to the zero pole cancellation. In other words, when the sensor is attached at any of the system nodes, some flexible modes will be unobservable [23].

2.1.2 Mechanical reflected waves

For the lumped inertial system shown in Fig.2.4, J_m and θ_m are the actuator inertia and angular position. The following equations of motion can be obtained

$$J_m\ddot{\theta}_m + B(\dot{\theta}_m - \dot{\theta}_1) + k(\theta_m - \theta_1) = \tau_m \tag{2.4}$$

$$J_1\ddot{\theta}_1 - B(\dot{\theta}_m - \dot{\theta}_1) - k(\theta_m - \theta_1) + B(\dot{\theta}_1 - \dot{\theta}_2) + k(\theta_1 - \theta_2) = 0 \tag{2.5}$$

13
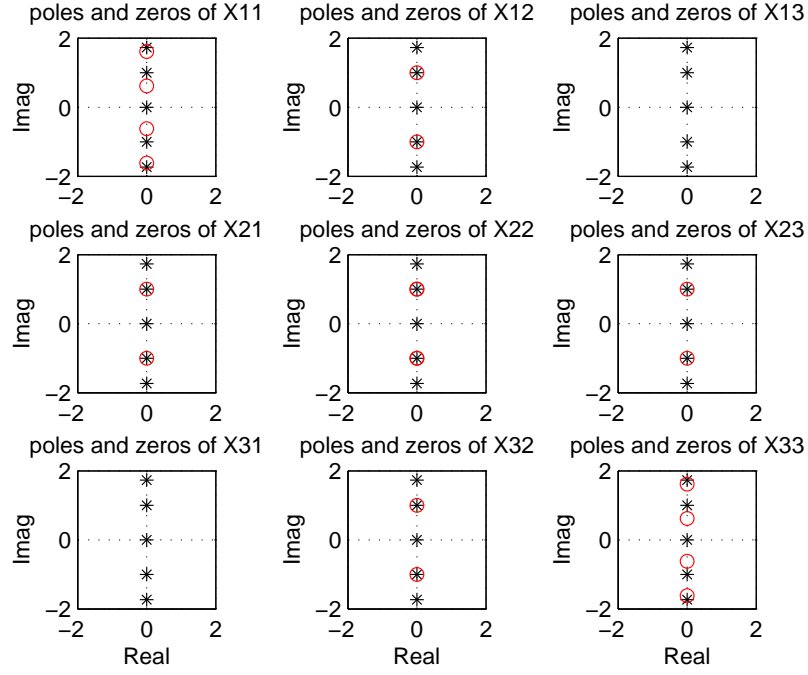
Figure 2.2: Poles and zeros for nine transfer functions, for $B_1 = B_2 = 0$

$$J_2\ddot{\theta}_2 - B(\dot{\theta}_1 - \dot{\theta}_2) - k(\theta_1 - \theta_2) + B(\dot{\theta}_2 - \dot{\theta}_3) + k(\theta_2 - \theta_3) = 0 \qquad (2.6)$$

$$\vdots$$

$$J_n\ddot{\theta}_n - B(\dot{\theta}_{n-1} - \dot{\theta}_n) - k(\theta_{n-1} - \theta_n) = 0. \qquad (2.7)$$

Putting it all together and solving for $B(\dot{\theta}_m - \dot{\theta}_1) + k(\theta_m - \theta_1)$ we get

$$B(\dot{\theta}_m - \dot{\theta}_1) + k(\theta_m - \theta_1) = J_1\ddot{\theta}_1 + J_2\ddot{\theta}_2 + J_3\ddot{\theta}_3 + \ldots + J_n\ddot{\theta}_n. \qquad (2.8)$$

Making the following definition

$$\tau_{ref} \triangleq B(\dot{\theta}_m - \dot{\theta}_1) + k(\theta_m - \theta_1) \qquad (2.9)$$

from Eq.2.8 we can rewrite the previous definition as

$$\tau_{ref} \triangleq J_1\ddot{\theta}_1 + J_2\ddot{\theta}_2 + J_3\ddot{\theta}_3 + \ldots + J_n\ddot{\theta}_n \qquad (2.10)$$

where τ_{ref} is the reflected torque from the mechanical system on the actuator. Usually it is defined as the mechanical load or disturbance on the actuator. Majority of

14
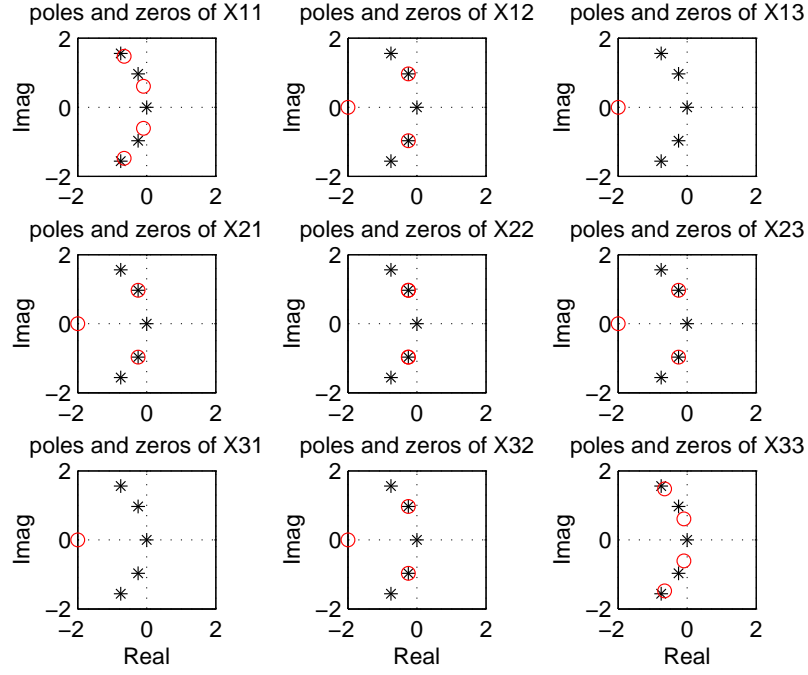
Figure 2.3: Poles and zeros for nine transfer functions, for $B_1 = B_2 = 0.5$
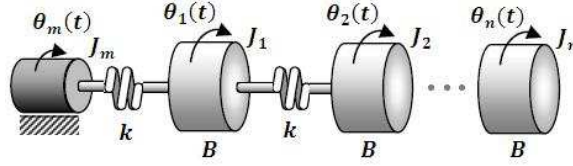
Figure 2.4: Lumped inertial system with uniform parameters

researchers and authors are estimating this term and along with other terms, and rejecting them by additional control term in order to obtain robust motion control. In this work, the mechanical load is defined as a reflected mechanical wave from the system as it carries all the systems dynamics and can be interpreted from Eq.2.10, or the system's uniform parameters as it can be interpreted from Eq.2.9. Similarly, it can be shown for a linear flexible lumped system that the reflected force wave is

$$f_{ref} \triangleq B(\dot{x}_m - \dot{x}_1) + k(x_m - x_1) \tag{2.11}$$

or

$$f_{ref} \triangleq m_1\ddot{x}_1 + m_2\ddot{x}_2 + m_3\ddot{x}_3 + \ldots + m_n\ddot{x}_n \tag{2.12}$$

15

for a system with externally applied torque or force due to the interaction with the environment. The equations of motion are

$$J_m\ddot{\theta}_m + B(\dot{\theta}_m - \dot{\theta}_1) + k(\theta_m - \theta_1) = \tau_m$$

$$J_1\ddot{\theta}_1 - B(\dot{\theta}_m - \dot{\theta}_1) - k(\theta_m - \theta_1) + B(\dot{\theta}_1 - \dot{\theta}_2) + k(\theta_1 - \theta_2) = \tau_{ext_1} \qquad (2.13)$$

$$J_2\ddot{\theta}_2 - B(\dot{\theta}_1 - \dot{\theta}_2) - k(\theta_1 - \theta_2) + B(\dot{\theta}_2 - \dot{\theta}_3) + k(\theta_2 - \theta_3) = \tau_{ext_2} \qquad (2.14)$$

$$\vdots$$

$$J_n\ddot{\theta}_n - B(\dot{\theta}_{n-1} - \dot{\theta}_n) - k(\theta_{n-1} - \theta_n) = \tau_{ext_n} \qquad (2.15)$$

where τ_{ext_i} is the external disturbance torque applied on the ith mass. The reflected torque wave in this case is

$$\tau_{ref} \triangleq \sum_{i=1}^{n} J_i\ddot{\theta}_i - \sum_{i=1}^{n} \tau_{ext_i} \triangleq B(\dot{\theta}_m - \dot{\theta}_1) + k(\theta_m - \theta_1). \qquad (2.16)$$

Surprisingly enough, the reflected force f_{ref} or torque τ_{ref} can be estimated from the actuator side using its current and velocity that will be explained in Chapter 3. In this section, it was shown that the reflected torque wave τ_{ref} carries all the flexible system's dynamics, uniform system's parameters and the externally applied forces or torques.

2.1.3 Mechanical wave propagation

In the previous section, reflected torque wave τ_{ref} was shown to carry all the flexible system's information back to the actuator side. In this section, we investigate whether the reflected waves are reflected and reconstructed at the actuator side. Therefore, the wave equation has to be solved and the solution has to be interpreted. The one dimensional wave equation is given as follows [24]

$$\frac{\partial^2 u(x,t)}{\partial t^2} + B\frac{\partial u(x,t)}{\partial t} - c^2\frac{\partial^2 u(x,t)}{\partial x^2} = H(t,x) \qquad (2.17)$$

16

$$c = \sqrt{\frac{G}{\rho}}$$

where B, c and $H(t, x)$ are the damping coefficient, wave propagation speed and the input forcing function, respectively. G and ρ are the modulus of rigidity and density of the media. Neglecting the damping term and rewriting the homogenous and forced equations

$$\frac{\partial^2 v(x, t)}{\partial t^2} - c^2 \frac{\partial^2 v(x, t)}{\partial x^2} = 0 \tag{2.18}$$

and

$$\frac{\partial^2 w(x, t)}{\partial t^2} - c^2 \frac{\partial^2 w(x, t)}{\partial x^2} = H(t, x) \tag{2.19}$$

the total response can be obtained by the superposition of the forced and natural responses

$$u(t, x) = v(t, x) + w(t, x). \tag{2.20}$$

The solutions of the forced and homogenous equations are included in Appendix.A.

$$u(t, x) = \frac{1}{2}[f(x + ct) + f(x - ct)] + R + S \tag{2.21}$$

$$R \triangleq f(x - ct)] + \frac{1}{2c}[\int_{x-ct}^{x+ct} g(s)ds]$$

$$S \triangleq \frac{1}{2c} \int_o^t \int_{x-c(\tau-t)}^{x+c(\tau+t)} H(s, \tau)ds d\tau$$

where $g(s)$ and $f(x)$ are the wave's initial velocity and configuration. $f(x - ct)$ represents a portion of $f(x)$ moving in one direction, while $f(x + ct)$ represents the other portion of $f(x)$ that is moving in the opposite direction as shown in Fig.2.5. Eq.2.21 indicates that the initial configuration of the wave that can be shaped by the initial forcing function splints into two equal portions moving with the same speed in opposite directions. Furthermore, the equation indicates that these two portions will reconstruct each other again at the system's boundaries. Therefore, we conclude that regardless of the splinting action that occurs to the wave when it is initiated, it will recover at two positions of the flexible system. These two positions are the system's
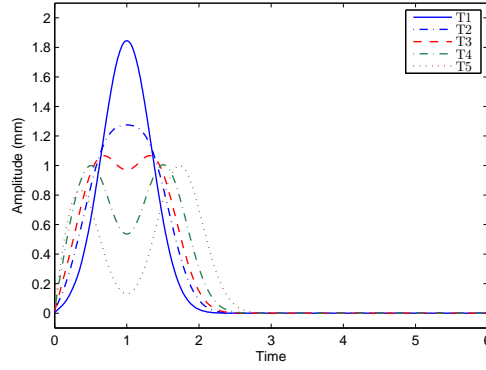
Figure 2.5: Simulation of the wave equation's solution $(T_1 < \ldots < T_5)$

boundaries where an actuator is located. Thus, reflected waves are accessible from the actuator side.

2.1.4 Transfer function interpretation

The wave equation's solution obtained in the previous section can be interpreted by driving the transfer function that maps the motion of each mass with its neighbor. Fig.2.6 illustrates a uniform mass spring system where the position of each i^{th}mass is related to the i^{i+1} by the following relation [3]

$$X_{i+1}(s) = G(s)X_i(s). \tag{2.22}$$
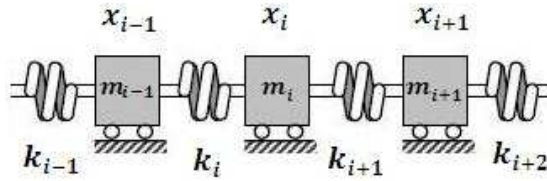
Figure 2.6: Uniform mass spring system

The equation of motion for the ith mass is

$$m\ddot{x}_i = k(x_{i-1} - 2x_i + x_{i+1}). \tag{2.23}$$

18

Taking Laplace transform of Eq.2.23, we get the following quadratic equation in $G(s)$

$$G^2(s) - (ms^2 + 2k)G(s) + k = 0. \tag{2.24}$$

Solving the quadratic equation we get

$$G_1(s) = 1 + \frac{1}{2}\frac{s^2}{2\omega_n^2} - \sqrt{\frac{s^2}{2\omega_n^2}(1 + \frac{s^2}{2\omega_n^2})} \tag{2.25}$$

$$G_2(s) = 1 + \frac{1}{2}\frac{s^2}{2\omega_n^2} + \sqrt{\frac{s^2}{2\omega_n^2}(1 + \frac{s^2}{2\omega_n^2})}. \tag{2.26}$$

Therefore, the position of each lumped mass can be obtained by the superposition of two components of the form O'Connar [1]

$$X_i(s) = \alpha_i(s)G_1(s) + \beta_i(s)G_2(s) \tag{2.27}$$

where $\alpha_i(s)$ and $\beta_i(s)$ are arbitrary, and making the following definitions

$$\psi(x + vt) \triangleq \alpha_i(s)G_1(s)$$

$$\psi(x - vt) \triangleq \beta_i(s)G_2(s).$$

Finally, we obtain

$$X_i(s) = \psi(x - vt) + \psi(x + vt). \tag{2.28}$$

The physical interpretation of Eq.2.28 is that the $\psi(x - vt)$ component of $X_i(s)$ corresponds to motion propagating in the direction of increasing i, the motion whose source is to the left, and which manifests itself over time in successive masses to the right with a phase lag and finite magnitude ratio. On the other hand, the second component $\psi(x + vt)$ is noncausal in the direction of increasing i. It must correspond, therefore, to a component of the motion of mass $i + 1$ that is not caused by the rightward propagating component of the motion of mass i, but is rather associated with motion whose source is to the right.

Therefore, we conclude that at each ith mass there will appear a component of motion propagating rightward and another one propagating leftward O'Connar [4].

That is similar to the interpretation of Eq.2.21. In other words, waves along flexible systems are moving in opposite directions, they splint and they reconstruct each other again linearly at the system's boundaries where actuator is located. Therefore, mechanical waves are accessible from the actuator side.

2.2   Frequency Response Analysis

It is assumed that the flexible lumped system has a single input, with three degrees of freedom. Therefore, the number of distinct transfer functions drops to three, and can be obtained from Eq.2.2 as follows

$$
\begin{aligned}
\frac{\theta_1(s)}{f_1(s)} &= \frac{J^2 s^4 + 3Jks^2 + k^2}{J^3 s^6 + 4J^2 ks^4 + 3Jk^2 s^2} \\
\frac{\theta_2(s)}{f_1(s)} &= \frac{Jks^2 + k^2}{J^3 s^6 + 4J^2 ks^4 + 3Jk^2 s^2} \\
\frac{\theta_3(s)}{f_1(s)} &= \frac{k^2}{J^3 s^6 + 4J^2 ks^4 + 3Jk^2 s^2} \; .
\end{aligned}
\tag{2.29}
$$

Dividing Eq.2.29 by J^3 we get

$$
\begin{aligned}
\frac{\theta_1(s)}{f_1(s)} &= \frac{s^4 + 3\omega_n^2 s^2 + \omega_n^4}{Js^2(s^4 + 4\omega_n^2 s^2 + 3\omega_n^4)} \\
\frac{\theta_2(s)}{f_1(s)} &= \frac{\omega_n^2 s^2 + \omega_n^4}{Js^2(s^4 + 4\omega_n^2 s^2 + 3\omega_n^4)} \\
\frac{\theta_3(s)}{f_1(s)} &= \frac{\omega_n^4}{Js^2(s^4 + 4\omega_n^2 s^2 + 3\omega_n^4)}
\end{aligned}
\tag{2.30}
$$

where ω_n is the natural frequency of the flexible system

$$
\omega_n^2 = \frac{k}{J} \; .
\tag{2.31}
$$

By substituting s with $j\omega$ and analyzing the low and high frequency behavior

$$
s \implies j\omega.
$$

Low frequency behavior

$$
\frac{\theta_1(j\omega)}{f_1(j\omega)}\Big|_{\omega \ll \omega_n} = \frac{-1}{3J\omega^2}
\tag{2.32}
$$

20

At low frequencies, the rigid body motion of θ_1 is falling off at a rate of $\frac{-1}{\omega^2}$, and with a gain of $\frac{1}{3J}$.

$$\frac{\theta_2(j\omega)}{f_1(j\omega)}\big|_{\omega<<\omega_n} = \frac{-1}{3J\omega^2} \tag{2.33}$$

$$\frac{\theta_3(j\omega)}{f_1(j\omega)}\big|_{\omega<<\omega_n} = \frac{-1}{3J\omega^2} \tag{2.34}$$

High frequency behavior

$$\frac{\theta_1(j\omega)}{f_1(j\omega)}\big|_{\omega>>\omega_n} = \frac{-1}{J\omega^2} \tag{2.35}$$

At high frequencies, the rigid body motion of θ_1 is falling at a rate of $\frac{-1}{\omega^2}$, and with a gain of $\frac{1}{J}$.

$$\frac{\theta_2(j\omega)}{f_1(j\omega)}\big|_{\omega>>\omega_n} = \frac{k}{J^2\omega^4} \tag{2.36}$$

$$\frac{\theta_3(j\omega)}{f_1(j\omega)}\big|_{\omega>>\omega_n} = \frac{-k^2}{J^3\omega^6} \tag{2.37}$$

From Eq 2.33, Eq 2.34 and Eq 2.35, we conclude that at low frequency range we have a rigid body motion behavior, and at this frequency range the equations of motion can be written as follows

$$3J\frac{d^2\theta(t)}{dt^2} = \tau(t). \tag{2.38}$$

This result will be the first step in the algorithm proposed in this thesis in order to estimate the parameters and the positions in a sensorless manner. Fig.2.7 summarizes the frequency response of the 3 DOF flexible system.

2.3   Modal Analysis

2.3.1   Modal matrix derivation

In this section, modal analysis of a 3 DOF flexible lumped inertial system is investigated in order to understand the relative motion between the lumped masses at certain frequencies. Modal analysis is equivalent to the eigenvalue/eigenvector problem where eigenvalues represent the flexible system's natural frequencies, while the
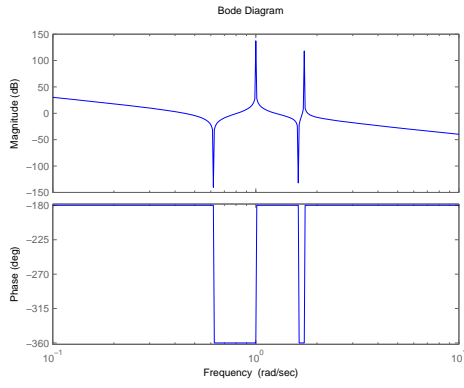
(a) First mass frequency response
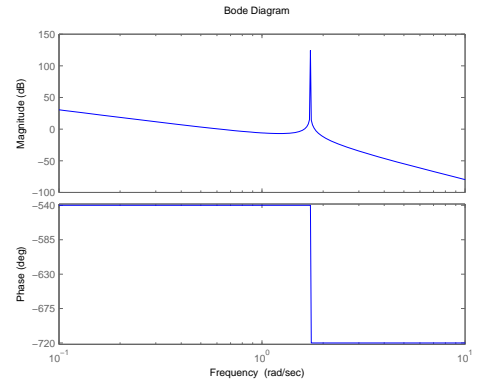
(b) Second mass frequency response
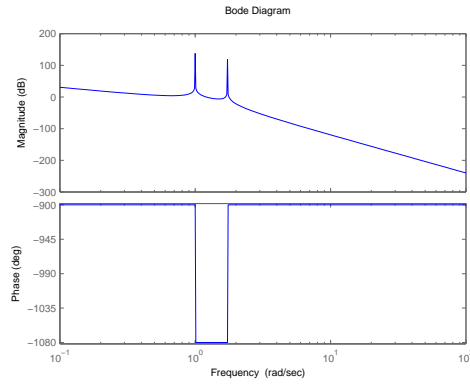
(c) Third mass frequency response

Figure 2.7: Flexible system's frequency responses

eigenvectors represent the modal vectors that describe the relative motion between system's degrees of freedom. The homogenous part of Eq.2.2 is

$$\mathbf{A} \, \boldsymbol{\Theta} = 0. \tag{2.39}$$

Solving the eigenvector problem assuming that damping coefficients are zero

$$\mathbf{A}\boldsymbol{\Theta} = \lambda\boldsymbol{\Theta}$$

$$(\mathbf{A} - \lambda\mathbf{I})\boldsymbol{\Theta} = 0 \ . \tag{2.40}$$

From the solution of the characteristic Eq.2.3 we get the eigenvalues $\lambda_1, \lambda_2 \ and \ \lambda_3$. Solving Eq.2.40 for $\lambda_1 = 0$

22

$$
\begin{bmatrix} k & -k & 0 \\ -k & 2k & -k \\ 0 & -k & k \end{bmatrix} \begin{bmatrix} \theta_1 \\ \theta_2 \\ \theta_3 \end{bmatrix} = \begin{bmatrix} 0 \\ 0 \\ 0 \end{bmatrix}
$$

we obtain the following eigenvector or modal vector

$$
\Theta_1 = \begin{bmatrix} 1 \\ 1 \\ 1 \end{bmatrix}. \tag{2.41}
$$

This implies that, at $0\ Hz$ flexible system is rigidly oscillating and the motion ratio between the masses is unity. Therefore, at this frequency a rigid body motion oscillation can be obtained and the flexible system is behaving rigidly.

For $\lambda_2 = j\sqrt{\frac{k}{m}}$

$$
\begin{bmatrix} -k & -k & 0 \\ -k & k & -k \\ 0 & -k & 0 \end{bmatrix} \begin{bmatrix} \theta_1 \\ \theta_2 \\ \theta_3 \end{bmatrix} = \begin{bmatrix} 0 \\ 0 \\ 0 \end{bmatrix}
$$

we obtain the following modal vector

$$
\Theta_2 = \begin{bmatrix} 1 \\ 0 \\ -1 \end{bmatrix}. \tag{2.42}
$$

This implies that at $\sqrt{\frac{k}{m}}\ Hz$, second mass is not moving with respect to the first mass, while first and third masses have the same amplitude and are out of phase.

For $\lambda_3 = j\sqrt{\frac{3k}{m}}$

$$
\begin{bmatrix} -2k & -k & 0 \\ -k & -k & -k \\ 0 & -k & -2k \end{bmatrix} \begin{bmatrix} x_1 \\ x_2 \\ x_3 \end{bmatrix} = \begin{bmatrix} 0 \\ 0 \\ 0 \end{bmatrix}
$$

23

the modal vector is

$$\mathbf{\Theta}_3 = \begin{bmatrix} 1 \\ -2 \\ 1 \end{bmatrix}. \tag{2.43}$$

This implies that at $\sqrt{\frac{3k}{m}} \, Hz$, the first and third masses have the same amplitude and are in phase, while the second mass's amplitude is twice the first mass's amplitude and are out of phase. Concatenating the previous modal vectors together we obtain

$$\mathbf{M} = [\mathbf{\Theta}_1|\mathbf{\Theta}_2|\mathbf{\Theta}_3]$$

$$\mathbf{M} = \begin{bmatrix} 1 & 1 & 1 \\ 1 & 0 & -2 \\ 1 & -1 & 1 \end{bmatrix} \tag{2.44}$$

where $\mathbf{M}^1$ is the modal matrix of the 3 DOF flexible system, that summarizes the relative motion between the lumped masses at certain frequencies.

2.3.2 Experimental interpretation of the modal matrix

In order to interpret the physical meaning of the previous modal matrix, the following experiment was performed on a three degree-of-freedom inertial flexible system. Experimental parameters are shown in Table.2.1.

The frequency of the forcing function was tuned between 0.1 rad/sec and 30 rad/sec. Fig.2.8 shows the oscillation of the three lumped masses for an arbitrary forcing function with a 1 rad/sec frequency. The masses have the same amplitude and are in phase, that is equivalent to the unit eigenvector in the modal matrix. Figure.2.9 indicates that the middle mass's amplitude is very low, while the other masses have the same amplitude and are out of phase, that is equivalent to the second modal vector where the second element of the second modal vector is zero and

---

[1]The modal matrix's elements are not necessarily integers, the obtained modal matrix is computed under the assumption of equal masses, spring constants and damping coefficients.

Table 2.1: Modal matrix experimental parameters

Parameter	Value	Parameter	Value
J_1	5152.99 gcm^2	J_3	6192.707 gcm^2
J_2	5152.99 gcm^2	f_{input}	[0.1-30]rad/sec

(a) systems oscillation

(b) Mag plot of a
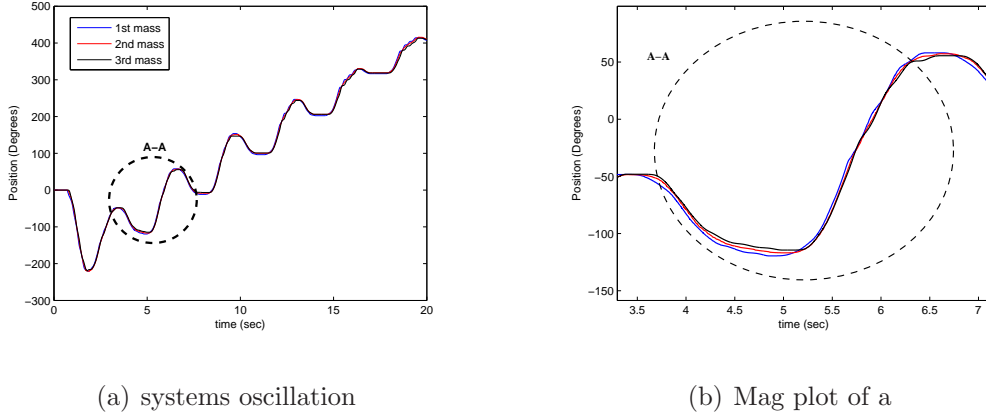
Figure 2.8: First eigenvector interpretation-f_{input}=1 rad/sec

the first and third are unity with opposite signs. Figure.2.10 shows that the middle mass is oscillating with twice the amplitude of the first and third masses and is out of phase, while both of them are in phase with the same amplitude, that is equivalent to the third eigenvector of the modal matrix. From the previous experiment we can conclude that the eigenvalues of the flexible lumped system are

$$\lambda_2 \simeq 12 rad/sec \quad (2.45)$$

$$\lambda_3 \simeq 22 rad/sec \ .$$

The frequency range of the rigid body oscillations falls below 5 rad/sec. In other words, all the masses of the system will be oscillating with the same amplitude and will be in phase if the frequency of the forcing function is kept below 5 rad/sec. Therefore, if the flexible system is required to be moving rigidly, the frequency of the forcing function has to be kept below 5 rad/sec for this particular system. Otherwise, any of the system's flexible modes will be excited and masses will be moving with

25
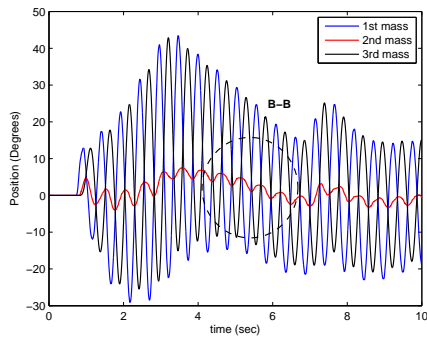
(a) systems oscillation
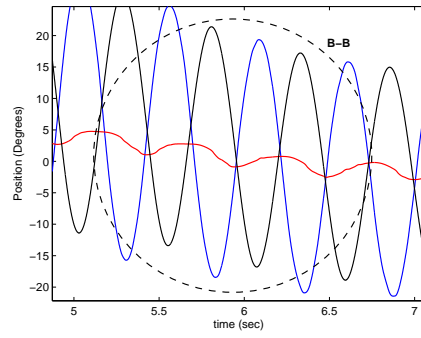
(b) Mag plot of a

Figure 2.9: Second eigenvector interpretation-f_{input}=11 rad/sec

different ratios with respect to each other.
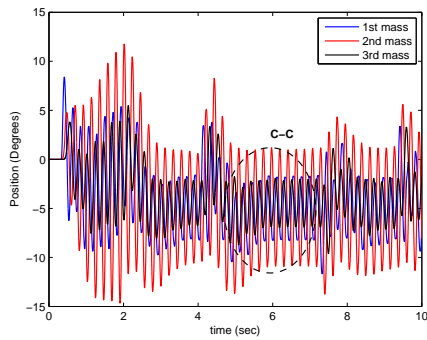
(a) systems oscillation
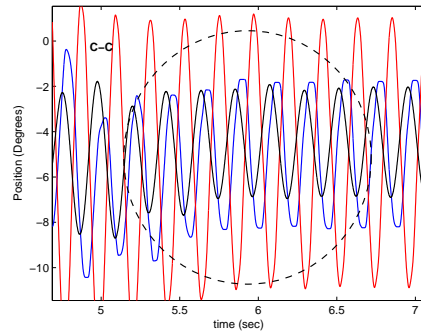
(b) Mag plot of a

Figure 2.10: Third eigenvector interpretation-f_{input}=22 rad/sec

CHAPTER 3

Sensorless Motion Control

The word 'sensorless' means that the flexible system is free from any attached sensors or measurement. It does not mean that we are not using any measurement, since one must sense or measure some variables to obtain some information as the basis of estimating the unknown variables. Only two variables are required to be measured from the actuator side, actuator's current and velocity. In this chapter an estimation algorithm is proposed based on these two measurements to estimate system parameters, observe the system's flexible motion and external disturbances or torques.

3.1 Reflected Torque Wave Estimation

Linear systems have the following state space representation, if the disturbance on the system is assumed to be added to the input side

$$\dot{x} = Ax + bu + ed$$
$$y = cx$$

$$(3.1)$$

where x is a state vector, A is a system matrix, b is the distribution vector of the input, e is a distribution vector of the disturbance, and c is the observation column vector. Considering the parameter variation

$$A = A_o + \triangle A$$
$$b = b_o + \triangle b$$

$$(3.2)$$

where $\triangle A$ and $\triangle b$ are the variation between the system's actual parameters A, b

27

and the system's nominal parameters A_o, b_o. The new state space equations are

$$\dot{x} = (A_o + \triangle A)x + (b_o + \triangle b)u + ed \qquad (3.3)$$

$$= A_o x + b_o u + (\triangle Ax + \triangle bu + ed)$$

where the third term of the right hand side of Eq.3.3 represent the disturbance input due to both parameter variation and the external forces on the system

$$\tilde{d} \triangleq \triangle Ax + \triangle bu + ed . \qquad (3.4)$$

Applying the previous equations on an actuator attached to inertial load as shown in Fig.3.1
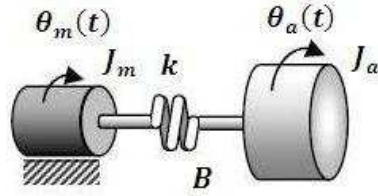
(a) Actuator with inertial load
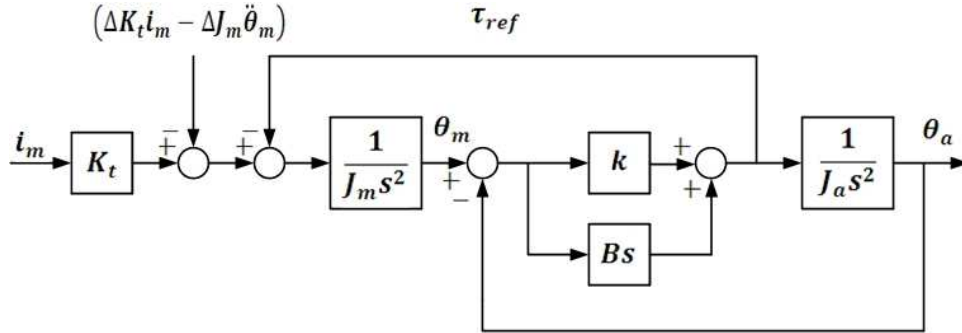
(b) Block diagram of the actuator and inertial load

Figure 3.1: Disturbance and reflected torque on the actuator side

$$L\frac{di_m}{dt} + Ri_m = k_t i_m - k_b \frac{d\theta_m}{dt} \qquad (3.5)$$

$$J_m \frac{d^2\theta_m}{dt^2} = k_t i_m - B(\dot{\theta}_m - \dot{\theta}_a) - k(\theta_m - \theta_a) . \qquad (3.6)$$

Considering the parameter's variation, where J_m and k_t are the actuator inertia and torque constant, J_{mo} and k_{to} are the nominal ones, while $\triangle J_m$ and $\triangle k_t$ are the

28

variations between the actual and nominal parameters

$$J_m = J_{mo} + \triangle J_m \tag{3.7}$$

$$k_t = k_{to} + \triangle k_t .$$

Eq.3.6 becomes

$$(J_{mo} + \triangle J_m)\frac{d^2\theta_m}{dt^2} = (k_t + \triangle k_{to})i_m - B(\dot{\theta}_m - \dot{\theta}_a) - k(\theta_m - \theta_a) . \tag{3.8}$$

For systems with coulomb friction f_{cm}

$$(J_{mo} + \triangle J_m)\frac{d^2\theta_m}{dt^2} = (k_t + \triangle k_{to})i_m - B(\dot{\theta}_m - \dot{\theta}_a) - k(\theta_m - \theta_a) - f_{cm} . \tag{3.9}$$

Re-arranging the terms

$$J_{mo}\frac{d^2\theta_m}{dt^2} = k_{to}i_m - B(\dot{\theta}_m - \dot{\theta}_a) - k(\theta_m - \theta_a) - f_{cm} + \triangle k_{to}i_m - \triangle J_m\frac{d^2\theta_m}{dt^2} . \tag{3.10}$$

Defining the total disturbance d on the actuator as

$$d \triangleq -f_{cm} - B(\dot{\theta}_m - \dot{\theta}_a) - k(\theta_m - \theta_a) + \triangle k_{to}i_m - \triangle J_m\frac{d^2\theta_m}{dt^2} \tag{3.11}$$

rewriting Eq.3.11

$$J_{mo}\frac{d^2\theta_m}{dt^2} = k_{to}i_m + d . \tag{3.12}$$

Eq.3.12 indicates that the disturbance on the actuator can be determined using the actuator's parameters and nominal values of the motor inertia and torque constants as follows

$$d = J_{mo}\frac{d^2\theta_m}{dt^2} - k_{to}i_m .$$

By estimating d through a low pass filter

$$\widehat{d} = \frac{g_{dist}}{s + g_{dist}}[J_{mo}\ddot{\theta}_m - i_a k_{to}] \tag{3.13}$$

where g_{dist} is a constant observer gain. the error between the actual disturbance and the estimated one is

$$\widetilde{d} = \widehat{d} - d . \tag{3.14}$$

Introducing Eq.3.12 and Eq.3.13. into Eq.3.14

$$\widetilde{d} = [J_{mo}\ddot{\theta}_m - i_a k_{to}]\frac{g_{dist}}{s + g_{dist}} - J_m\ddot{\theta}_m + i_a k_t \ . \tag{3.15}$$

Multiplying Eq.3.15 by $(s + g_{dist})$ yields

$$\begin{aligned} s\widetilde{d} + g_{dist}\widetilde{d} &= g(j_{mo} - j_m)\ddot{\theta}_m - sJ_m\ddot{\theta}_m + g(k_t - k_{to})i_a + si_a k_t \tag{3.16} \\ &= g_{dist}\triangle J\ddot{\theta}_m - sJ_m\ddot{\theta}_m + gk_t i_a + si_a k_t \ . \end{aligned}$$

By defining the right hand side as

$$\xi \triangleq g_{dist}\triangle J\ddot{\theta}_m - sJ_m\ddot{\theta}_m + gk_t i_a + si_a k_t$$

and rewriting Eq.3.16 in the standard first order differential equation form

$$\frac{d}{dt}\widetilde{d} + g_{dist}\widetilde{d} = \xi \ . \tag{3.17}$$

Eq.3.17 describes the estimation error dynamics, solving the previous differential equation for $\widetilde{d}$ we get

$$\widetilde{d}(t) = e^{-g_{dist}t}\int_o^t e^{g_{dist}t}\ \xi\ d\tau + ce^{-g_{dist}t} \ . \tag{3.18}$$

Therefore, we conclude that as $t \Longrightarrow \infty$ the estimation error $\widetilde{d} \Longrightarrow 0$ thus $\widehat{d} \Longrightarrow d$. The convergence ratio may be increased by changing the low pass filter gain g_{dist}. In other words, the disturbance is estimated through the first order low pass filter shown in Fig.3.2.a. Since the numerical differentiation of the speed signal may result in high level of noise in the calculated acceleration signal, The direct differentiation is avoided by using the disturbance observer configuration shown in Fig.3.2.b. Toshiaki [12]

$$t \longmapsto \infty \Longrightarrow \widetilde{d} \longmapsto 0$$

$$\widetilde{d} \longmapsto 0 \Longrightarrow \widehat{d} \longmapsto d$$

Rewriting Eq.3.11 and using the estimate of the disturbance instead of the actual

(a) Direct differentiation configuration   (b) Indirect differentiation configuration
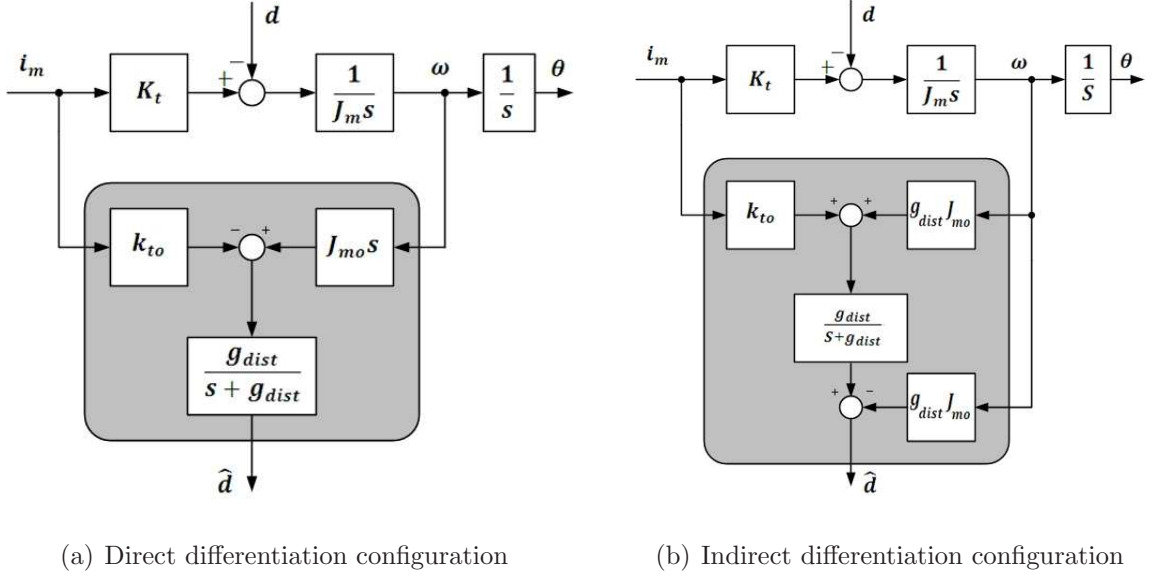
Figure 3.2: Disturbance observer structure

one

$$d \Longrightarrow \widehat{d}$$

$$\widehat{d} = -f_{cm} - B(\dot{\theta}_m - \dot{\theta}_a) - k(\theta_m - \theta_a) + \triangle k_{to} i_m - \triangle J_m \frac{d^2\theta_m}{dt^2} \; . \tag{3.19}$$

Recalling Eq.2.16 that describes the reflected torque wave

$$\tau_{ref} = \sum_{i=1}^{n} J_i \ddot{\theta}_i - \sum_{i=1}^{n} \tau_{ext_i} = B(\dot{\theta}_m - \dot{\theta}_1) + k(\theta_m - \theta_1) \; . \tag{3.20}$$

It turns out that, the estimated disturbance d includes the reflected torque wave τ_{ref}, the varied self-inertia torque $\triangle J_m \frac{d^2\theta_m}{dt^2}$, torque ripple from the actuator $\triangle k_{to} i_m$ and the coulomb friction torque f_{cm}. Eq.3.19 can be written as follows

$$\widehat{d} = -f_{cm} - \tau_{ref} + \triangle k_{to} i_m - \triangle J_m \frac{d^2\theta_m}{dt^2} \; . \tag{3.21}$$

The reflected torque wave τ_{ref} has to be decoupled out of the total disturbance d. Therefore, both the torque ripple of the actuator $\triangle k_{to} i_m$ and the varied self-inertia torque $\triangle J_m \frac{d^2\theta_m}{dt^2}$ have to be determined or estimated and the disturbance observer shown in Fig.3.2 has to be modified so that the reflected torque can be decoupled from other terms of Eq.3.19.

31

3.1.1 Parameters's variation disturbance estimation

In order to decouple the reflected torque τ_{ref} out of the estimated disturbance $\widehat{d}$, the parameters's variation disturbance have to be estimated or determined first. Assuming that the actuator is free from any attached inertial loads, the actuator's mechanical dynamics is described as

$$J_m \frac{d^2\theta_m}{dt^2} = k_t i_m - d_{par} \tag{3.22}$$

where d_{par} is the disturbance due to the parameteres's variations and the viscous friction torque, that is given as

$$d_{par} = -B\dot{\theta}_m + \triangle k_t i_m - \triangle J_m \frac{d^2\theta_m}{dt^2} . \tag{3.23}$$

Other terms of Eq.3.19 are dropped, as the actuator is running free from any attached load. Since d_{par} can be estimated using the actuator's current and velocity, Eq.3.23 becomes

$$\widehat{\underline{d}}_{par} = -B\dot{\underline{\theta}}_m + \triangle k_{to}\underline{i}_m - \triangle J_m\ddot{\underline{\theta}}_m \tag{3.24}$$

where $\widehat{\underline{d}}_{par}$ is the estimated parameters's disturbance data point vector, while $\dot{\underline{\theta}}_m$, $\ddot{\underline{\theta}}_m$ and $\underline{i}_m$ are data point vectors of actuator's velocity, acceleration and current. Putting Eq.3.24 in matrix form as follows

$$\begin{bmatrix} \triangle k_t & -B & -\triangle J_m \end{bmatrix}_{1\times 3} \begin{bmatrix} \underline{i}_m \\ \dot{\underline{\theta}}_m \\ \ddot{\underline{\theta}}_m \end{bmatrix}_{3\times r} = \begin{bmatrix} \widehat{\underline{d}}_{par} \end{bmatrix}_{r\times 1} \tag{3.25}$$

where r is the number of data points, defining

$$H \triangleq \begin{bmatrix} \underline{i}_m \\ \dot{\underline{\theta}}_m \\ \ddot{\underline{\theta}}_m \end{bmatrix} .$$

Rewriting Eq.3.25

$$\begin{bmatrix} \triangle k_t & -B & -\triangle J_m \end{bmatrix} H = \begin{bmatrix} \widehat{\underline{d}}_{par} \end{bmatrix} .$$

Eq.3.25 describes an over-determined system, where the number of equations are greater than the number of unknowns. Thus, solution of such systems have to minimize some cost functions such as the norm square of errors. Therefore, the estimates of the parameters's variation disturbance can be computed as follows

$$\left[\begin{array}{ccc} \widehat{\triangle k_t} & -\widehat{B} & -\widehat{\triangle J_m} \end{array}\right] = \left[\begin{array}{c} H^T H \end{array}\right]^{-1} H^T \left[\begin{array}{c} \widehat{d}_{par} \end{array}\right] \qquad (3.26)$$

or

$$\left[\begin{array}{ccc} \widehat{\triangle k_t} & -\widehat{B} & -\widehat{\triangle J_m} \end{array}\right] = \mathbf{H}^\dagger \left[\begin{array}{c} \widehat{d}_{par} \end{array}\right] \qquad (3.27)$$

where $\mathbf{H}^\dagger$ is the pseudo-inverse of H. $\widehat{\triangle k_t}$ and $\widehat{\triangle J_m}$ are the estimated actuator's torque ripple and varied self-inertia torque, respectively.

3.1.2 Reflected torque wave decoupling

As the parameters's variation disturbance are estimated by Eq.3.27, they can be used in order to decouple the reflected torque wave τ_{ref} from the total disturbance d by adding the estimates of the parameters's variation estimates to both sides of Eq.3.21 and neglecting the coulomb friction torque

$$-\widehat{\triangle k_t}\ i_m + \widehat{\triangle J_m}\ \ddot{\theta}_m + \widehat{d} = -\tau_{ref} + \triangle k_t i_m - \triangle J_m \ddot{\theta}_m - \widehat{\triangle k_t}\ i_m + \widehat{\triangle J_m}\ \ddot{\theta}_m \qquad (3.28)$$

$$\widehat{\triangle k_t}\ i_m + \widehat{\triangle J_m}\ \ddot{\theta}_m + \widehat{d} = -\tau_{ref} + (\triangle k_t - \widehat{\triangle k_t})i_m + (\widehat{\triangle J_m} - \triangle J_m)\ddot{\theta}_m\ .$$

And since

$$\widehat{\triangle J_m} \simeq \triangle J_m$$

$$\widehat{\triangle k_t} \simeq \triangle k_t$$

the estimate of the reflected torque is

$$\widehat{\tau}_{ref} = \widehat{\triangle k_t}\ i_m - \widehat{\triangle J_m}\ \ddot{\theta}_m - \widehat{d}\ . \qquad (3.29)$$

The block diagram implementation of Eq.3.29 is shown in Fig.3.3, where the direct

(a) Direct differentiation configuration   (b) Indirect differentiation configuration
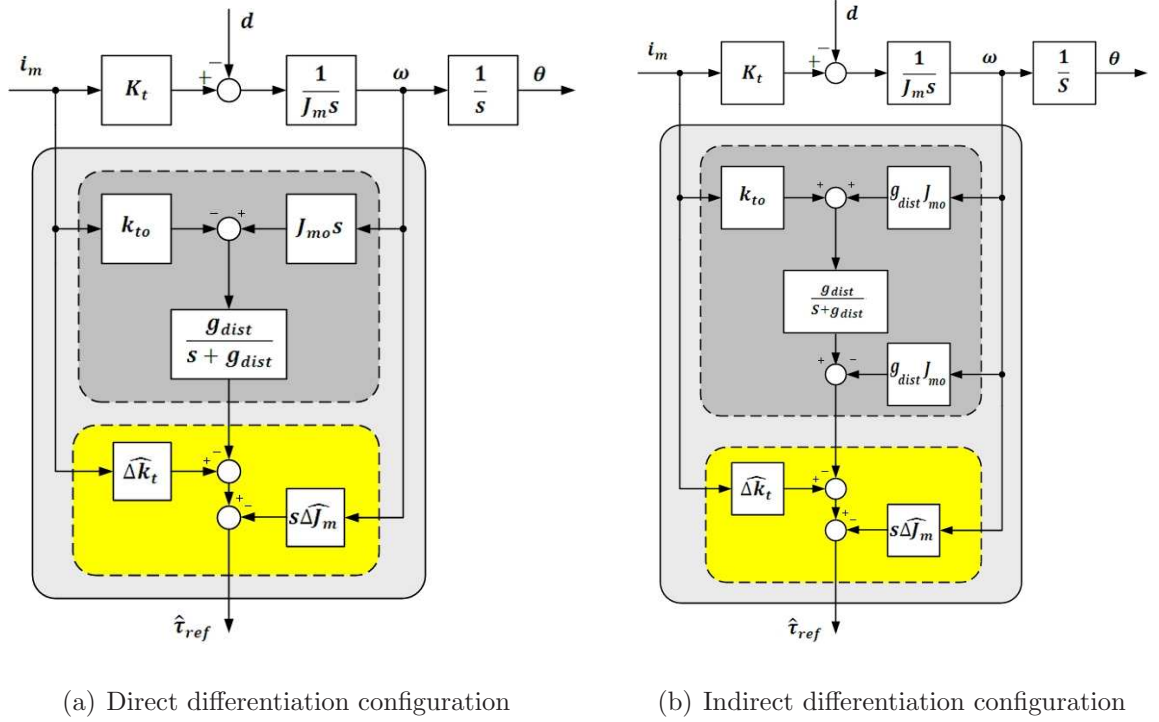
Figure 3.3: Reflected torque observer structure

differentiation is not avoided in the configuration shown in Fig.3.3.a. The other configuration shown in Fig.3.3.b also requires the differentiation of the velocity signal. Therefore, the reflected torque wave observer shown in Fig.3.3 will result in high level of noise amplification in the estimated reflected torque wave $\widehat{\tau}_{ref}$. In order estimate the reflected torque wave with minimum level of noise amplification the structure of the observer has to be modified as follows

$$\widehat{\tau}_{ref} = \frac{g_{ref}}{s + g_{ref}}[i_m \widehat{\triangle k_t} - \widehat{d} + g_{ref}\widehat{\triangle J_m}\dot{\theta}_m] - g_{ref}\widehat{\triangle J_m}\dot{\theta}_m \qquad (3.30)$$

where g_{ref} is the observer's constant gain or the corner frequency of the low pass filter, $\widehat{d}$ is the estimated total disturbance. The reflected torque wave is estimated through a first order low pass filter as shown in Fig.3.4. without differentiating the velocity signal to keep the noise amplification level as low as possible.

The modified observer shown in Fig.3.4 can be used to provide:

1. Total disturbance estimate $\widehat{d}$
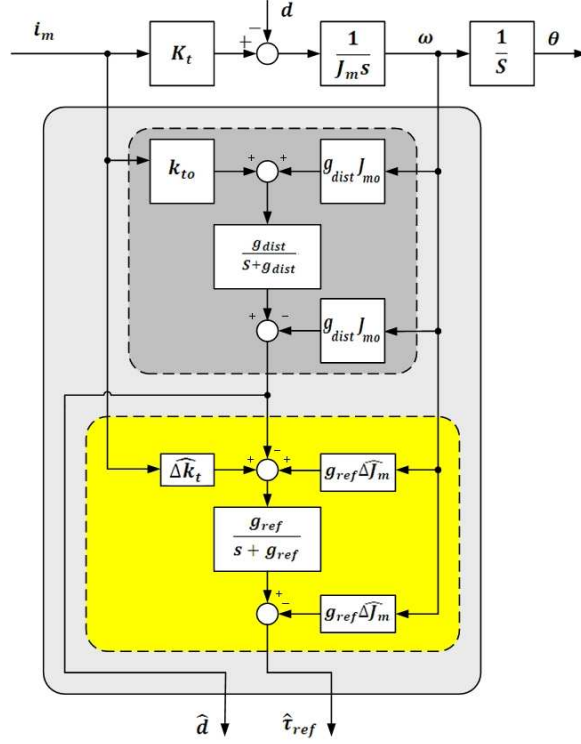
Figure 3.4: Modified reflected torque observer

2. Reflected torque estimate $\widehat{\tau}_{ref}$.

An off-line experiment is required to detect the parameter's variation disturbance using Eq.3.27 along with the actuator's current and velocity. The reflected torque by its turn is used to obtain[1]:

1. system's rigid motion estimate

2. system uniform parameters

3. system's flexible motions estimates

4. externally applied torques or disturbances estimates.

Indeed, the modification added to the conventional disturbance observer requires performing an off-line experiment, but the obtained outcomes make it possible to use

---

[1]The following items will be explained in the current chapter's following sections

the new observer in variety of applications. In other words, the modified observer can be used to accomplish robust motion control by rejecting the disturbance d, that can be achieved by adding a compensation current to the reference current as shown In Fig.3.5.
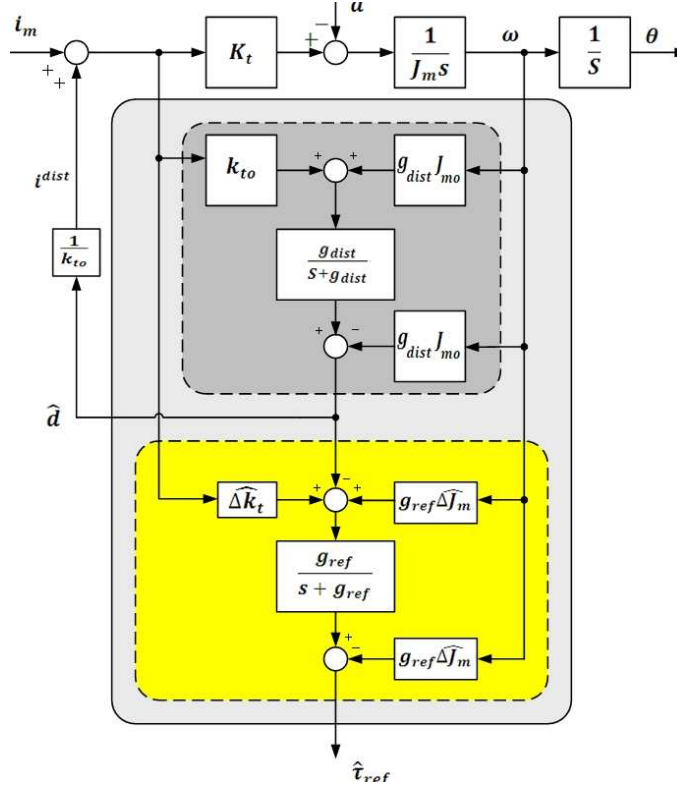
Figure 3.5: Modified observer-disturbance rejection

In addition to the disturbance rejection ability, the modified observer can be used to estimate the reflected torque wave, that is used along with the actuator parameters as the inputs of the sensorless estimation algorithm as it is illustrated in Fig.3.6

3.2 Rigid Body Motion Estimation

Modal and frequency response analysis of flexible lumped systems show that at low frequency range the flexible system is behaving as a rigid body. The ratios between all
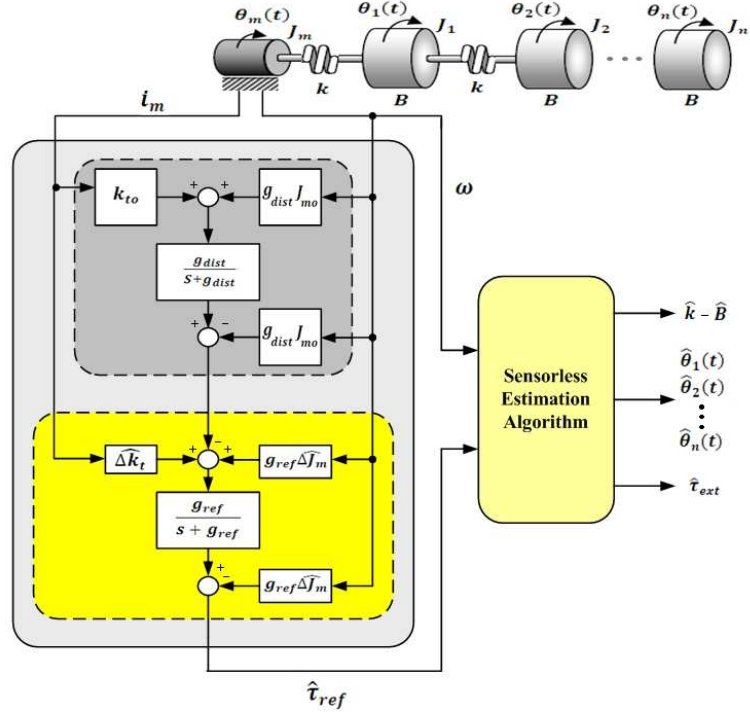
Figure 3.6: Modified observer-sensorless estimation

the masses' positions are unity as it was shown by the modal matrix M in Chapter.2

$$
\mathbf{M} = \begin{bmatrix} 1 & 1 & 1 \\ 1 & 0 & -2 \\ 1 & -1 & 1 \end{bmatrix}
$$

where the first vector represent the ratios of the masses' positions at a particular frequency. On the other hand, the second and third vectors of M represent flexible motion of the system at other particular frequencies. Recalling Eq.2.10 that describes the reflected torque of an n DOF flexible system

$$
\tau_{ref} = B(\dot{\theta}_m - \dot{\theta}_1) + k(\theta_m - \theta_1) = J_1\ddot{\theta}_1 + J_2\ddot{\theta}_2 + J_3\ddot{\theta}_3 + \ldots + J_n\ddot{\theta}_n . \tag{3.31}
$$

Where θ_1, θ_2 ... θ_n are the coordinates of the flexible system. For the second eigenvector of the modal matrix M, the angular position θ_2 is zero and so do the velocity and the acceleration, while the angular position θ_1 is equal to θ_3 with opposite sign.

The motion of the flexible system at the system's natural frequencies can be

summarized as follows

$$\Theta_2 = \begin{bmatrix} 1 \\ 1 \\ 1 \end{bmatrix}_{f_1 \ Hz} \implies \theta_1 = \theta_2 = \theta_3$$

$$\Theta_2 = \begin{bmatrix} 1 \\ 0 \\ -1 \end{bmatrix}_{f_2 \ Hz} \implies \theta_2 = 0 \ , \ \theta_1 = -\theta_3 \qquad (3.32)$$

$$\Theta_3 = \begin{bmatrix} 1 \\ 0 \\ -1 \end{bmatrix}_{f_3 \ Hz} \implies \theta_2 = -2\theta_1, \ \theta_1 = \theta_3 \ .$$

It turns out that, if the forcing function has zero energy at the system's resonant frequencies, flexible system will be oscillating rigidly and consequently single degree of freedom will be enough to describe the motion of the flexible system. In other words, if any of the system's flexible modes are excited, n coordinates have to be determined in order to describe the motion of the system. On the other hand, single coordinate is enough to describe the rigid motion of the flexible system that is no longer flexible. Therefore, if any of the system's flexible modes is not excited along with the assumption that all the lumped inertial masses have equal initial position and velocity

$$\theta_1(t_o) = \theta_2(t_o) = \theta_3(t_o) = \ldots = \theta_n(t_o)$$
$$\dot{\theta}_1(t_o) = \dot{\theta}_2(t_o) = \dot{\theta}_3(t_o) = \ldots = \dot{\theta}_n(t_o)$$

we conclude that

$$\theta_1(t) = \theta_2(t) = \theta_3(t) = \ldots = \theta_n(t) \qquad (3.33)$$

that is only valid in a narrow region of the system's frequency range, providing that the previous initial conditions are similar.

3.2.1 Filtering and/or fourier synthesis the control input

One way to keep the control input free from any energy at the system's resonance frequencies, is to pre-filer the control input with a low-pass filter. The low-pass filter will guarantee that the control input will not excite any of the system's flexible modes. The low-pass filter's corner frequency has to be chosen according to the modal analysis of the system. For example, the corner frequency of the low-pass filter for a system with the parameters given in Table.2.1 is about 3 rad/sec. Another way to excite the system's rigid mode, is Fourier synthesis of the control input such that the sinusoidal signals that construct the input have zero energy at the system's resonant frequencies. Threfore, the control input can be constructed as follows

$$u(t) = A_o + \sum_{k=1}^{N} (\frac{1}{2} A_k e^{j\phi_k} e^{j2\pi f_k t} + \frac{1}{2} A_k e^{-j\phi_k} e^{-j2\pi f_k t}) \mid_{f_k \neq f_{res}} \qquad (3.34)$$

where f_k is the frequency of the sinusoidal signals that build the control input, f_{res} are the system's resonance frequencies, A_k and A_o are the sinusoidal signals's amplitudes and Dc offset, respectively. In order to guarantee that the control input $u(t)$ will not excite any of the system's flexible modes, f_k should not coincide with f_{res}. The control input condition of Eq.3.34 along with the equal initial position and velocity assumption make it possible to rewrite Eq.3.31 as follows

$$\tau_{ref} = \ddot{\theta}(J_1 + J_2 + J_3 + \ldots + J_n) \qquad (3.35)$$

where θ is the angular position of the entire flexible system that is no longer flexible as Eq.3.34 is satisfied. Replacing the actual reflected torque by the estimated one, results in an estimate of the rigid body position $\widehat{\theta}$

$$\tau_{ref} \longrightarrow \widehat{\tau}_{ref} \Longrightarrow \theta \longrightarrow \widehat{\theta}$$

that can be computed by the following equation

$$\widehat{\theta}(t) = \frac{1}{\sum_{i=1}^{n} J_i} \int_o^t \int_o^t \widehat{\tau}_{ref} d\tau d\tau + c_1 t + c_2 \qquad (3.36)$$

where c_1 and c_2 are the integration constants. Similarly, the position estimate for a linear flexible system is

$$\widehat{x}(t) = \frac{1}{\sum_{i=1}^{n} m_i} \int_o^t \int_o^t \widehat{f}_{ref} d\tau d\tau + c_1 t + c_2 . \qquad (3.37)$$

Fig.3.7 shows the block diagram representation of the rigid body motion estimation.
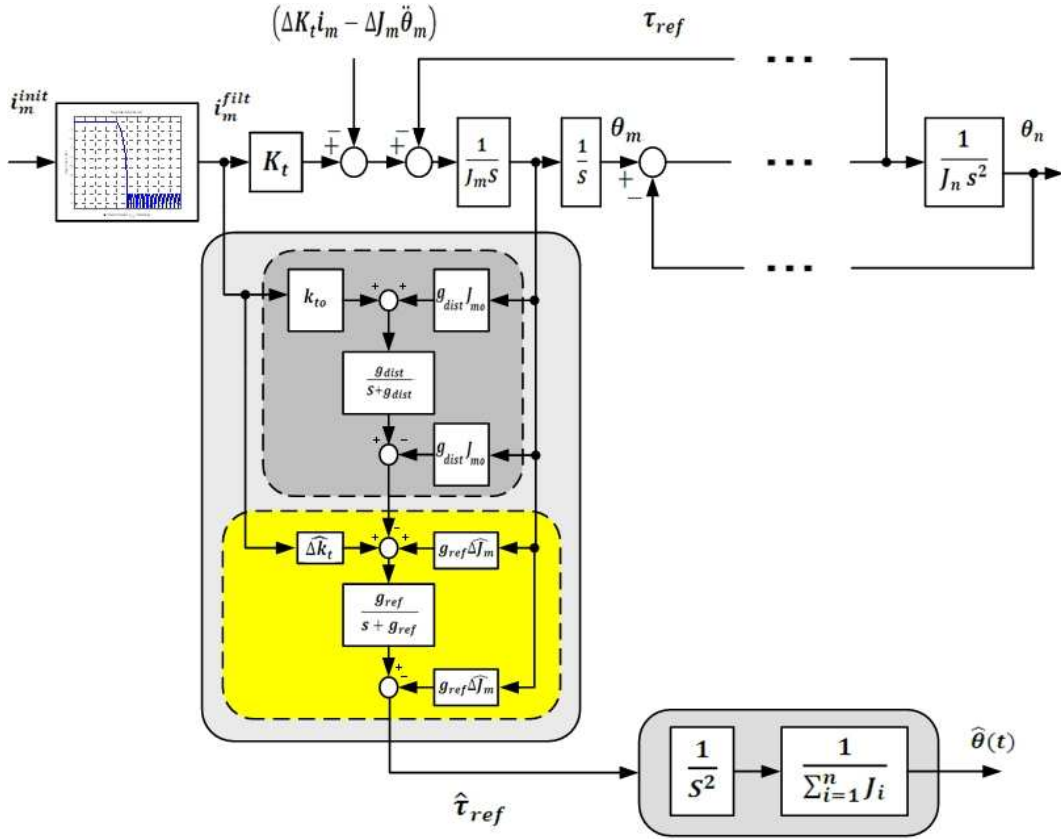
Figure 3.7: Rigid motion estimation

Firstly, the control input is filtered using a low-pass filter to guarantee the rigid mode excitation, then the reflected disturbance is estimated using the actuator's current and velocity. An off-line experiment is needed to estimate the parameter's variation disturbance used in the estimation of the reflected torque wave that allows estimating the rigid body motion of the flexible system without taking any measurement from the flexible system's side. Estimation of the rigid body motion is a step toward the estimation of system's flexible motion.

3.3 Parameters Estimation

Since the reflected torque wave is given by Eq.3.31 as follows

$$\tau_{ref} = B(\dot{\theta}_m - \dot{\theta}) + k(\theta_m - \theta) \ .$$

Replacing the actual reflected torque τ_{ref} with it's estimate $\widehat{\tau}_{ref}$, and the system's rigid position θ with it's estimate $\widehat{\theta}$

$$\widehat{\tau}_{ref} = B(\dot{\theta}_m - \dot{\widehat{\theta}}) + k(\theta_m - \widehat{\theta}) \tag{3.38}$$

and defining the velocity and position differences as

$$\underline{\xi} \triangleq (\theta_m - \widehat{\theta})$$

$$\underline{\eta} \triangleq (\dot{\theta}_m - \dot{\widehat{\theta}})$$

where $\underline{\xi}$ represents velocity difference data points vector, while $\underline{\eta}$ is the position difference data points vector. Similarly, $\widehat{\underline{\tau}}_{ref}$ is the estimated reflected torque data point vector. Rewriting Eq.3.38 in the following matrix form

$$\begin{bmatrix} \underline{\xi} & \underline{\eta} \end{bmatrix}_{n\times 2} \begin{bmatrix} k \\ B \end{bmatrix}_{2\times 1} = \begin{bmatrix} \widehat{\underline{\tau}}_{ref} \end{bmatrix}_{n\times 1} \ . \tag{3.39}$$

Eq.3.39 represents an over-determined system and the solution of the unknown system parameters vector has to minimize the norm square of errors. Therefore, the uniform stiffness and uniform damping coefficients can be found as follows

$$\mathbf{G} \triangleq \begin{bmatrix} \underline{\xi} & \underline{\eta} \end{bmatrix}$$

and the solution for the optimum system parameters is

$$\begin{bmatrix} \widehat{k} \\ \widehat{B} \end{bmatrix} = \begin{bmatrix} \mathbf{G}^T\mathbf{G} \end{bmatrix}^{-1} \mathbf{G}^T \begin{bmatrix} \widehat{\underline{\tau}}_{ref} \end{bmatrix} \tag{3.40}$$

$$\begin{bmatrix} \widehat{k} \\ \widehat{B} \end{bmatrix} = \mathbf{G}^\dagger \begin{bmatrix} \widehat{\underline{\tau}}_{ref} \end{bmatrix} \ . \tag{3.41}$$

Where $\mathbf{G}^{\dagger}$ is the pseudo inverse of $\mathbf{G}$, $\widehat{k}$ and $\widehat{B}$ are the estimates of the system's uniform stiffness and damping coefficient. Fig.3.8 shows the parameters estimation process, that is based on the actuator's parameters measurements. The previous procedures can be considered as another off-line experiment that has to be performed in order to determine the estimates of system parameters.
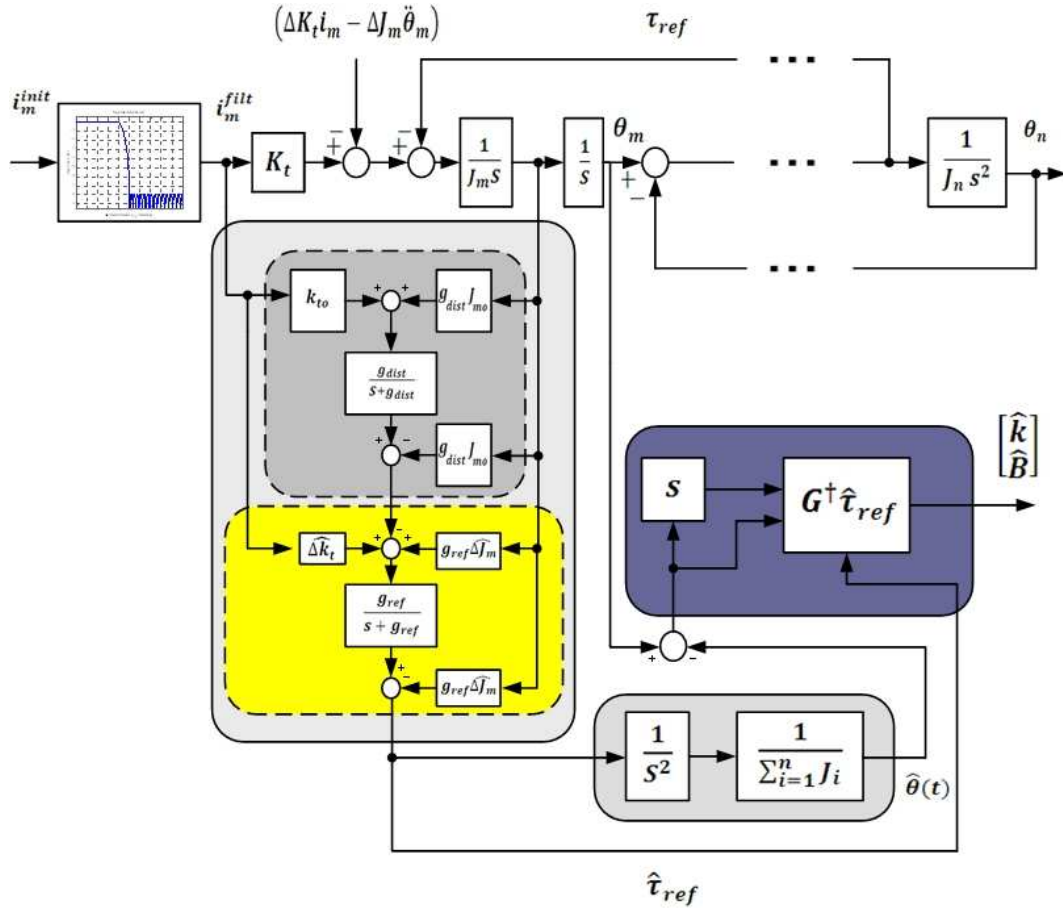
Figure 3.8: Parameters estimation

3.4   Flexible Motion Estimation

In the previous sections, rigid body motion is estimated using Eq.3.36 assuming that Eq.3.34 is satisfied and the initial velocities and positions were equal. But the rigid body motion does not represent the global behavior of the lumped masses at different

frequencies. It just represents the system's behavior at narrow region of the system's frequency range. Therefore, in this section the previous results such as the estimated reflected torque and the estimated parameters are used in order to determine the flexible motion of each lumped mass of the system regardless to the forcing function's frequency.

3.4.1   Recursive flexible motion estimation

Recalling Eq.3.38

$$\widehat{\tau}_{ref} = B(\dot{\theta}_m - \widehat{\dot{\theta}}) + k(\theta_m - \widehat{\theta})$$

and replacing the actual parameters with the estimated ones

$$B \Longrightarrow \widehat{B}$$

$$k \Longrightarrow \widehat{k}$$

we get

$$\widehat{\tau}_{ref} = \widehat{B}(\dot{\theta}_m - \widehat{\dot{\theta}}) + \widehat{k}(\theta_m - \widehat{\theta}) \ . \tag{3.42}$$

Re-arranging the terms

$$\widehat{B}\dot{\theta}_1 + \widehat{k}\theta_1 = \widehat{B}\dot{\theta}_o + \widehat{k}\theta_o - \widehat{\tau}_{ref} \tag{3.43}$$

and defining the right hand side as

$$\alpha \triangleq \widehat{B}\,\dot{\theta}_o + \widehat{k}\,\theta_o - \widehat{\tau}_{\mathbf{ref}} \ .$$

Solving the first order differential equation Eq.3.43 for $\widehat{\theta}_1(t)$ that[2] represents the position estimate of the first lumped inertial mass, we get

$$\widehat{\theta}_1(t) = e^{-\frac{\widehat{B}}{\widehat{k}}t} \int_o^t \beta e^{\frac{\widehat{B}}{\widehat{k}}\tau} d\tau + e^{-\frac{\widehat{B}}{\widehat{k}}t} c_1 \tag{3.44}$$

---

[2] $\theta_1(t)$ is based on the estimated reflected torque $\widehat{\tau}_{ref}$, estimated stiffness $\widehat{k}$ and estimated damping coefficient $\widehat{B}$. Therefore, its denoted as $\widehat{\theta}_1(t)$

where

$$\beta \triangleq \frac{\alpha}{\widehat{B}} \; .$$

The estimate of the second lumped position can be determined by solving the following differential equation for $\widehat{\theta}_2(t)$

$$\widehat{B} \; \dot{\theta}_2 + \widehat{k} \; \theta_2 = J_1 \widehat{\ddot{\theta}}_1 - \widehat{B}(\dot{\theta}_o - \widehat{\dot{\theta}}_1) - \widehat{k}(\theta_o - \theta_1) + \widehat{B} \; \widehat{\dot{\theta}}_1 + \widehat{k} \; \widehat{\theta}_1 \; . \tag{3.45}$$

Defining

$$\gamma \triangleq J_1 \widehat{\ddot{\theta}}_1 - \widehat{B}(\dot{\theta}_o - \widehat{\dot{\theta}}_1) - \widehat{k}(\theta_o - \theta_1) + \widehat{B} \; \widehat{\dot{\theta}}_1 + \widehat{k} \; \widehat{\theta}_1$$

we get the following solution

$$\widehat{\theta}_2(t) = e^{-\frac{\widehat{k}}{\widehat{B}}t} \int_o^t \zeta e^{\frac{\widehat{k}}{\widehat{B}}\tau} d\tau + e^{-\frac{\widehat{B}}{\widehat{k}}t} c_2 \tag{3.46}$$

where

$$\zeta \triangleq \frac{\gamma}{\widehat{B}} \; .$$

The estimate of the third lumped mass position is

$$\widehat{\theta}_3(t) = e^{-\frac{\widehat{k}}{\widehat{B}}t} \int_o^t \varepsilon \; e^{\frac{\widehat{k}}{\widehat{B}}\tau} d\tau + e^{-\frac{\widehat{B}}{\widehat{k}}t} c_3 \tag{3.47}$$

where

$$\varepsilon \triangleq \frac{\delta}{\widehat{B}}$$

$$\delta \triangleq J_2 \; \widehat{\ddot{\theta}}_2 - \widehat{B}(\widehat{\dot{\theta}}_1 - \widehat{\dot{\theta}}_2) - \widehat{k}(\widehat{\theta}_1 - \widehat{\theta}_2) + \widehat{B} \; \widehat{\dot{\theta}}_2 + \widehat{k} \; \widehat{\theta}_2 \; .$$

The estimate of the forth lumped mass position is

$$\widehat{\theta}_4(t) = e^{-\frac{\widehat{k}}{\widehat{B}}t} \int_o^t \varphi \; e^{\frac{\widehat{k}}{\widehat{B}}\tau} d\tau + e^{-\frac{\widehat{B}}{\widehat{k}}t} c_4 \tag{3.48}$$

where

$$\varphi \triangleq \frac{\phi}{\widehat{B}}$$

$$\phi \triangleq J_3 \; \widehat{\ddot{\theta}}_3 - \widehat{B}(\widehat{\dot{\theta}}_2 - \widehat{\dot{\theta}}_3) - \widehat{k}(\widehat{\theta}_2 - \widehat{\theta}_3) + \widehat{B} \; \widehat{\dot{\theta}}_3 + \widehat{k} \; \widehat{\theta}_3 \; .$$
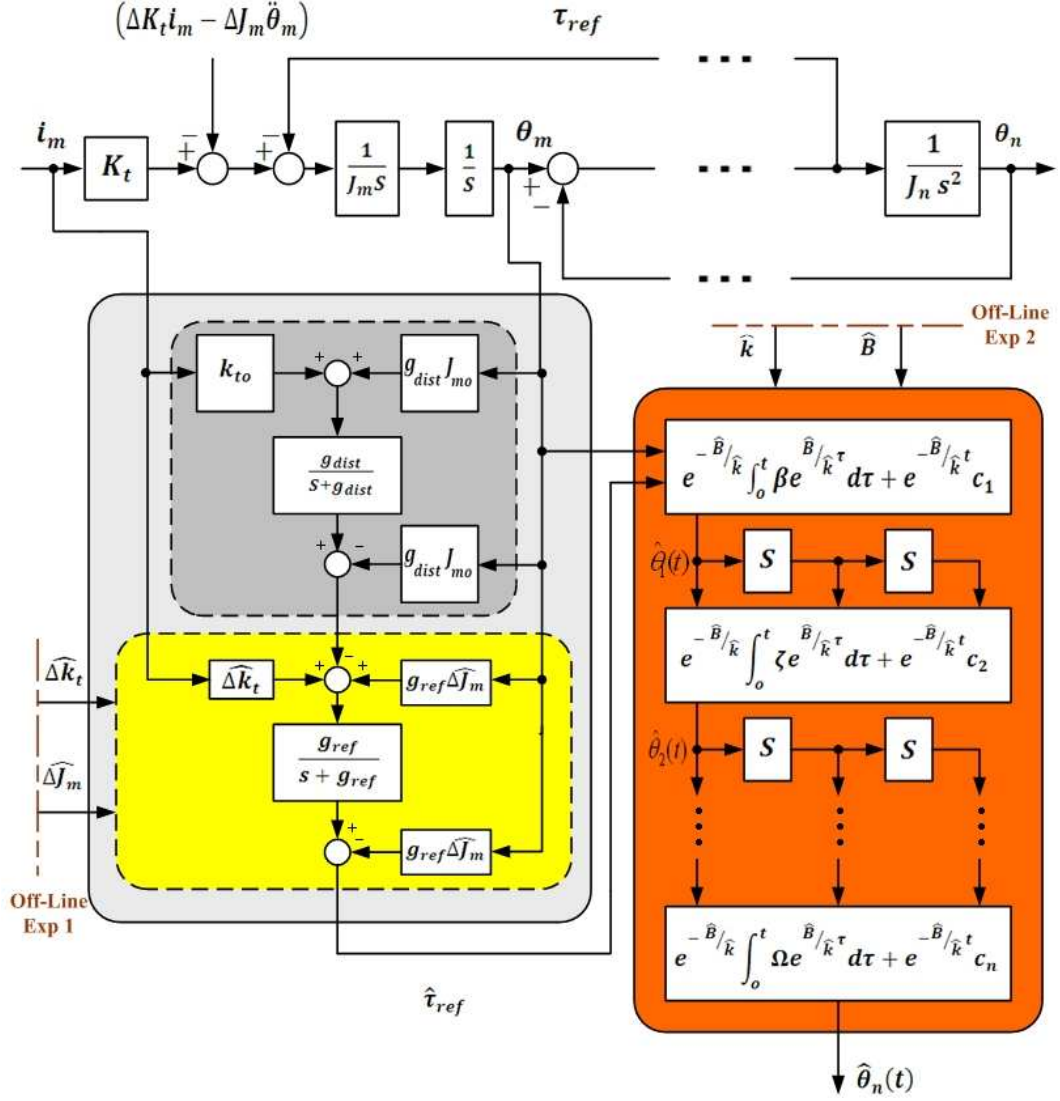
Figure 3.9: Flexible motion estimation

From the above equation we conclude that the estimates of the flexible lumped positions are determined in a recursive way and the entire process depends on a chain of estimators. Starting with the reflected torque estimation to the rigid body motion estimation, then estimating the system parameters and ending up with a recursive flexible motion estimation process.

In general, the estimate of the flexible lumped masses position is given by the following formula

$$\widehat{\theta}_i(t) = e^{-\frac{\widehat{k}}{\widehat{B}}t} \int_o^t \Omega \, e^{\frac{\widehat{k}}{\widehat{B}}\tau} d\tau + e^{-\frac{\widehat{B}}{\widehat{k}}t} c_i \tag{3.49}$$

where

$$\Omega \triangleq \frac{\Psi}{\widehat{B}}$$

$$\Psi \triangleq g(J_{i-1}, \widehat{\theta}_{i-1}, \widehat{\dot{\theta}}_{i-1}, \widehat{\ddot{\theta}}_{i-1}, \widehat{k}, \widehat{B}) \ .$$

Appendix.B includes the mathematical proof of the flexible lumped masses' positions estimation. The block diagram representation of the flexible motion estimation is shown in Fig.3.9. The position of each lumped mass has to be determined by a recursive manner. Two off-line experiments have to be performed before estimating the system's flexible motion. The first off-line experiment is to determine the actuator's self varied-inertia torque and the actuators torque ripple in order to decouple the estimated reflected torque out of the estimated disturbance, while the second off-line experiment is the uniform parameters estimation experiment that is used to estimate system uniform stiffness and damping coefficient.

3.5 External Disturbance Estimation

As the flexible system's dynamics and parameters are estimated, externally applied forces or torques can be determined using Eq.2.16. Using the available estimates instead of the actual variables and parameters we get

$$\widehat{\tau}_{ref} = \sum_{i=1}^{n} J_i \widehat{\ddot{\theta}}_i - \sum_{i=1}^{n} \tau_{ext_i} = \widehat{B}(\dot{\theta}_m - \widehat{\dot{\theta}}_1) + \widehat{k}(\theta_m - \widehat{\theta}_1) \tag{3.50}$$

therefore the estimate of the externally applied torque is

$$\widehat{\tau}_{ext} = \sum_{i=1}^{n} J_i \widehat{\ddot{\theta}}_i - \widehat{\tau}_{ref} \ . \tag{3.51}$$

Eq.3.51 indicates that the estimation of the external disturbances or torques due to the interaction with the environment requires the estimate of the reflected torque wave $\widehat{\tau}_{ref}$ along with all lumped masses' accelerations estimates.

The force estimation process is shown in Fig.3.10 where an external applied disturbance torque τ_{ext} is added due to the plant's interaction with the environment. In this
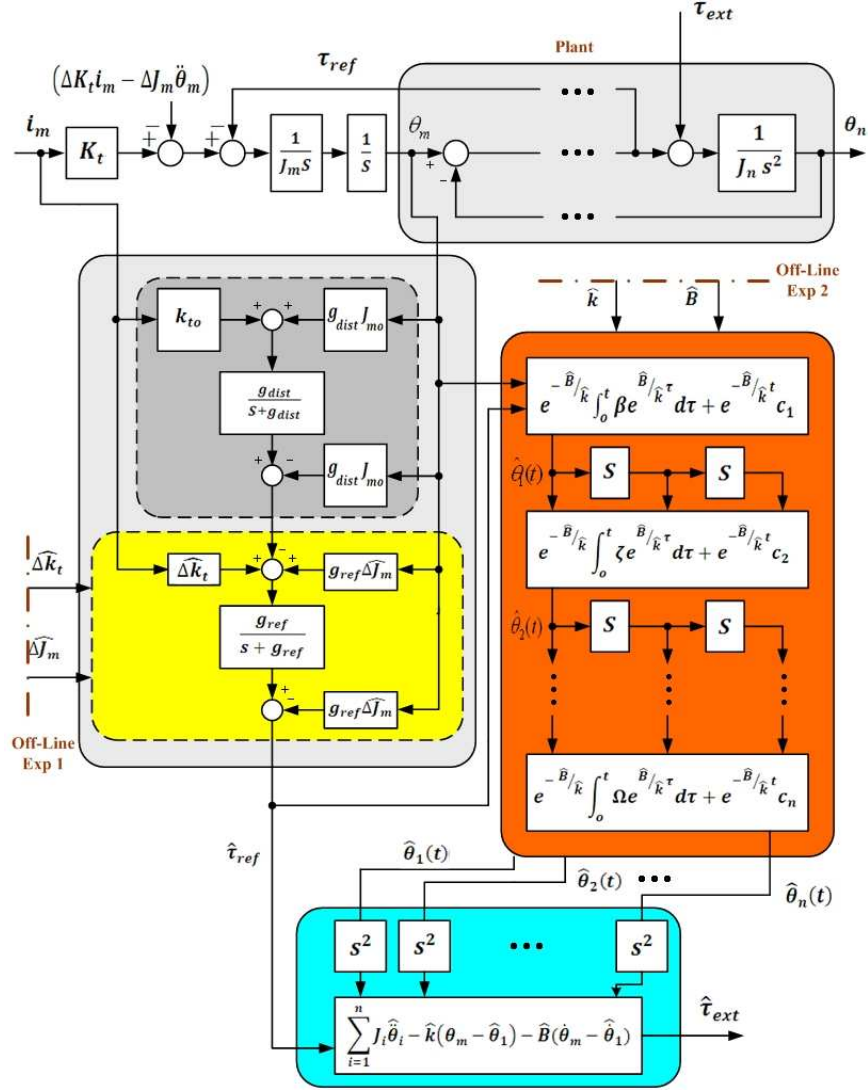
Figure 3.10: External applied torque estimation

case all the lumped positions have to be estimated using the recursive flexible motion estimation equations, and differentiated twice to obtain the masses' accelerations. Then the external applied torque is estimated using Eq.3.51.

Figure.3.10 shows a very interesting feature of the proposed algorithm where there are three types of disturbances added on the system:

1. The external disturbance on the plant τ_{ext}.

2. The reflected load or torque wave on the actuator τ_{ref}.

47

3. The parameters's variation disturbance $(\Delta k_t i_m - \Delta J_m \ddot{\theta}_m)$.

Each of these disturbances can be decoupled and used according to the required application. In other words, if robustness has to be achieved the total disturbance has to be estimated and rejected. If the external disturbance due to the interaction with the environment has to be determined, the previous chain of estimators have to be used keeping in mind that the required off-line experiments do not require any additional sensors or equipment. Only the actuator's velocity and current are measured and the necessary calculations are then performed.

3.6   Sensorless Motion Control

The availability of the lumped masses' positions estimates makes it possible to feedback these position estimates to the controller instead of the actual measurement. Since all the estimates are available and accessible, it is easier to control the position of any lumped mass of the system without attaching additional sensors or changing there locations as shown in Fig.3.11.

If the estimates are used as feedback instead of the actual measurements the error signal will be

$$\widehat{e}(t) = \theta_{ref}(t) - \widehat{\theta}_i(t) \tag{3.52}$$

If the first mass is required to be positioned to a certain reference θ_{ref}, the following sensorless control law can be used

$$u(t) = k_p(\theta_{ref} - \widehat{\theta}_1) + k_d(\dot{\theta}_{ref} - \widehat{\dot{\theta}}_1) \tag{3.53}$$

and if the disturbance has a significant impact on the results, the sensorless control law is

$$u(t) = k_p(\theta_{ref} - \widehat{\theta}_1) + k_d(\dot{\theta}_{ref} - \widehat{\dot{\theta}}_1) + i^{dist} \tag{3.54}$$
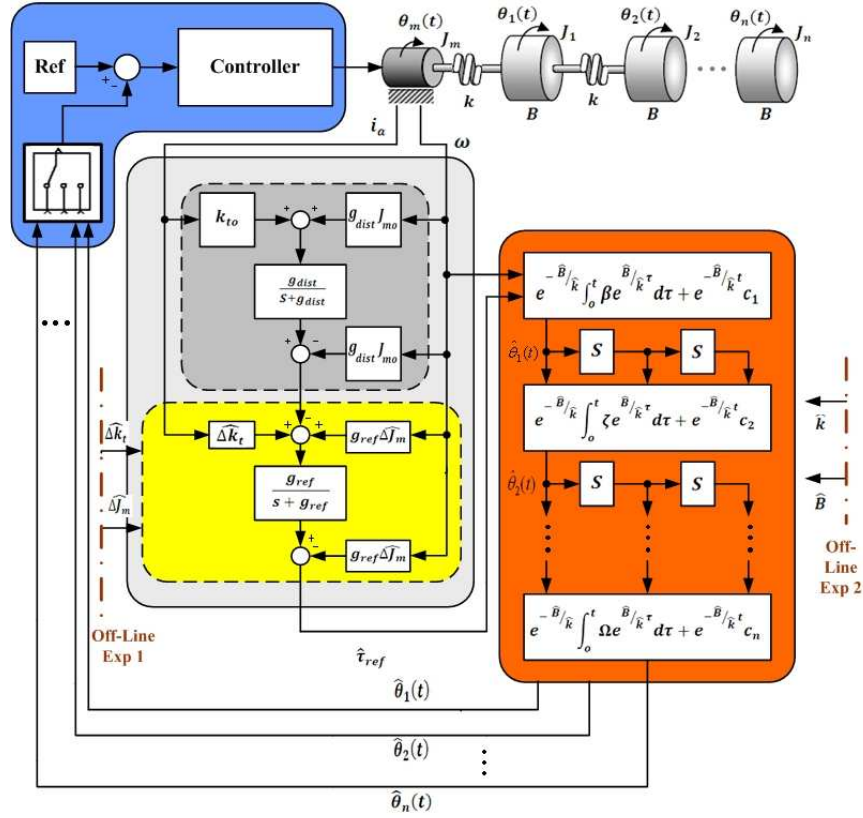
Figure 3.11: Sensorless motion control

where i^{dist} is a compensation input. Controlling the second mass requires feeding its position estimate back to the controller and the control law is

$$u(t) = k_p(\theta_{ref} - \widehat{\theta}_2) + k_d(\dot{\theta}_{ref} - \widehat{\dot{\theta}}_2) \qquad (3.55)$$

or

$$u(t) = k_p(\theta_{ref} - \widehat{\theta}_2) + k_d(\dot{\theta}_{ref} - \widehat{\dot{\theta}}_2) + i^{dist} . \qquad (3.56)$$

The control law for estimation based PID controller is

$$u(t) = k_p(\theta_{ref} - \widehat{\theta}_i) + k_d(\dot{\theta}_{ref} - \widehat{\dot{\theta}}_i) + k_i \int_0^t (\theta_{ref} - \widehat{\theta}_i) dt \qquad (3.57)$$

where k_p, k_i and k_d are the proportional, derivative and integral gains respectively. i is the index of the ith mass required to be controlled. The block diagram representation of Eq.3.57 is shown in Fig.3.12. The compensation input i^{dist} that has to be added

49
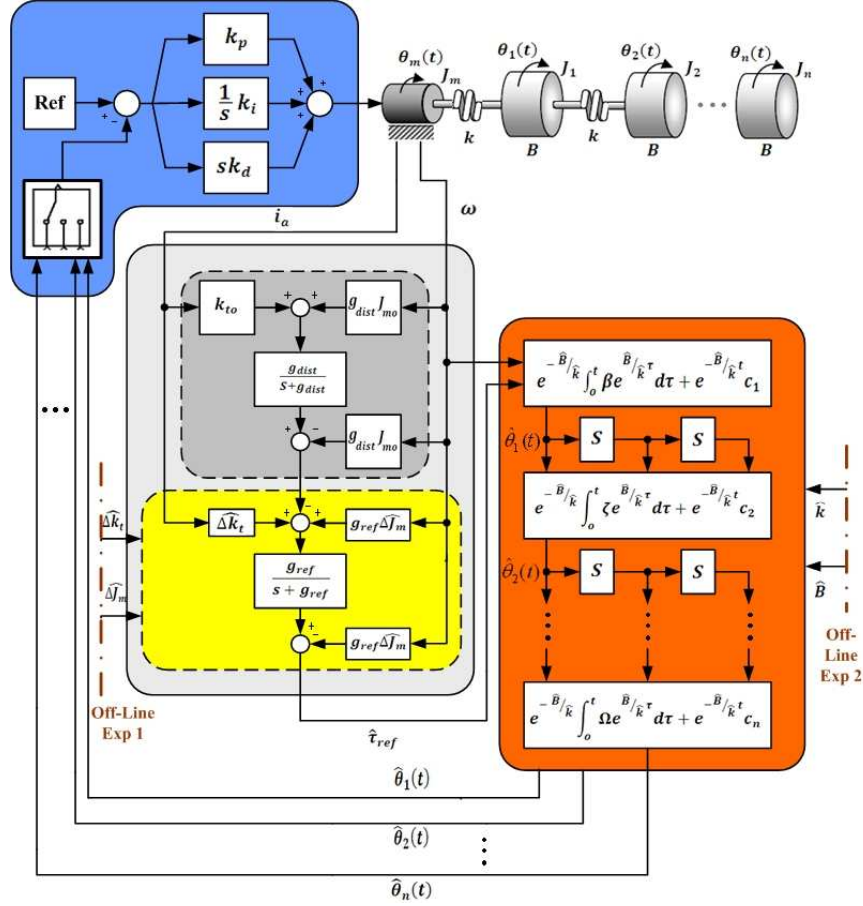
Figure 3.12: Estimation based PID controller

to the control input in order to reject the disturbances can be determined as follows

$$i^{dist} = \frac{1}{k_{to}}\widehat{d} \ . \tag{3.58}$$

the overall control law becomes

$$u(t) = k_p(\theta_{ref} - \widehat{\theta_i}) + k_d(\dot{\theta}_{ref} - \widehat{\dot{\theta}_i}) + k_i \int_0^t (\theta_{ref} - \widehat{\theta_i})dt + i^{dist} \ . \tag{3.59}$$

The block diagram representation of Eq.3.59 is shown in Fig.3.13 that shows an interesting feature of the modified disturbance observer or the other torque observer added to the conventional disturbance observer where the outputs of each observer are treated differently. Firstly, the output of the disturbance observer is the total disturbance on the actuator side and can be used to accomplish robust motion control, while the output of the torque observer is the reflected torque wave, that is used as
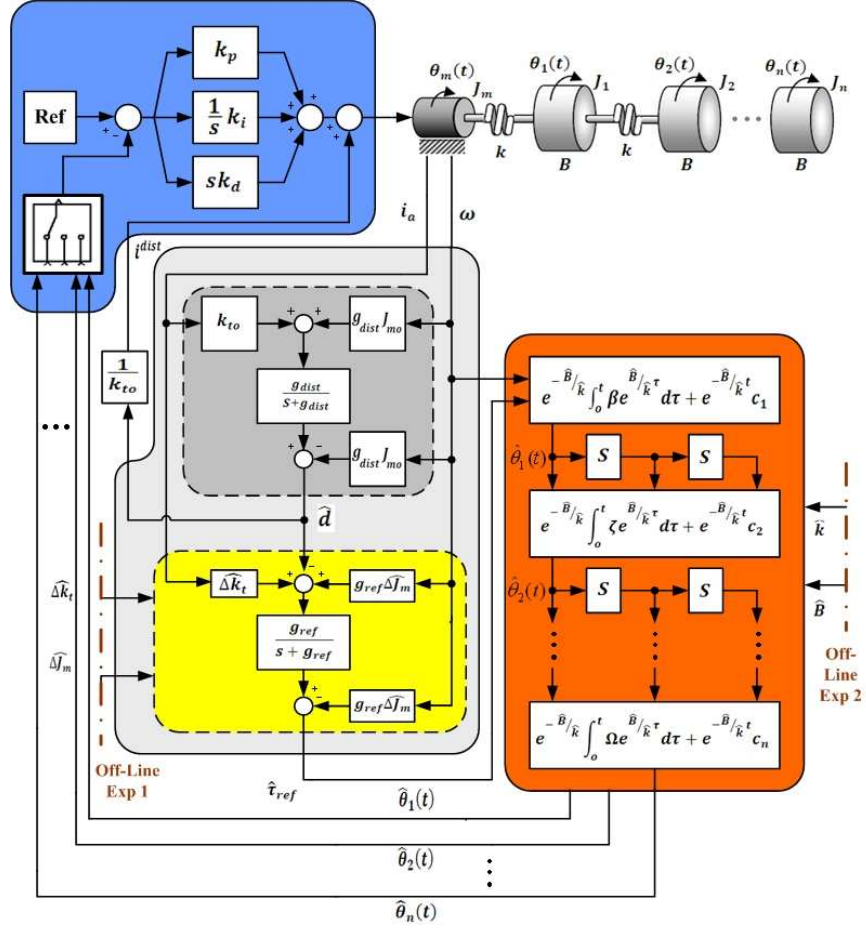
Figure 3.13: Estimation based PID controller with disturbance rejection

an input for further estimation processes such as parameters estimation and motion estimation. In other words, modifying the structure of the disturbance observer makes it possible not only to achieve robust motion control but also to analyze the reflected torque wave from the actuator platform.

3.7 The Entire Sensorless Estimation Algorithm Summary

3.7.1 Off-line experiment 1

Off-line experiment-1 is performed in order to determine the actuator's parameters variation disturbances $\triangle J_m$ and $\triangle k_t$. Figure.3.14 shows an illustration of the experiment.

The experimental procedures are:

1. Keeping the actuator free from any attached loads.

2. Measuring the actuators current and velocity from the unloaded actuator.

3. Estimating the disturbance using Eq.3.24.

4. Determine the actuator parameters variation disturbance using Eq.3.27.
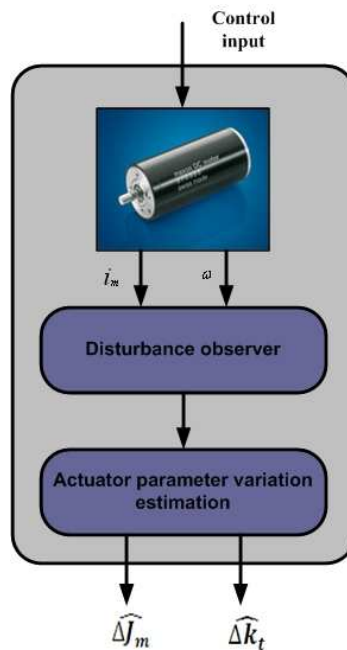
Figure 3.14: Off-line experiment 1

3.7.2 Off-line experiment 2

Off-line experiment-2 is performed in order to determine the system uniform parameters such as stiffness and the damping coefficient. Figure.3.15 shows an illustration of the experiment.

The experimental procedures are:

1. Connecting the flexible system to the actuator.

2. Filtering and/or Fourier synthesize the initial forcing function using equation.3.34 or the results obtained from the Modal analysis experiment.

3. Measuring the actuator's current and velocity.

4. Estimating the disturbance using Eq.3.13.

5. Estimating the reflected torque using Eq.3.30 along with the parameters obtained from off-line experiment 1

6. Estimating the system's rigid motion using. Eq.3.36

7. Determine the uniform system parameters using. Eq.3.41
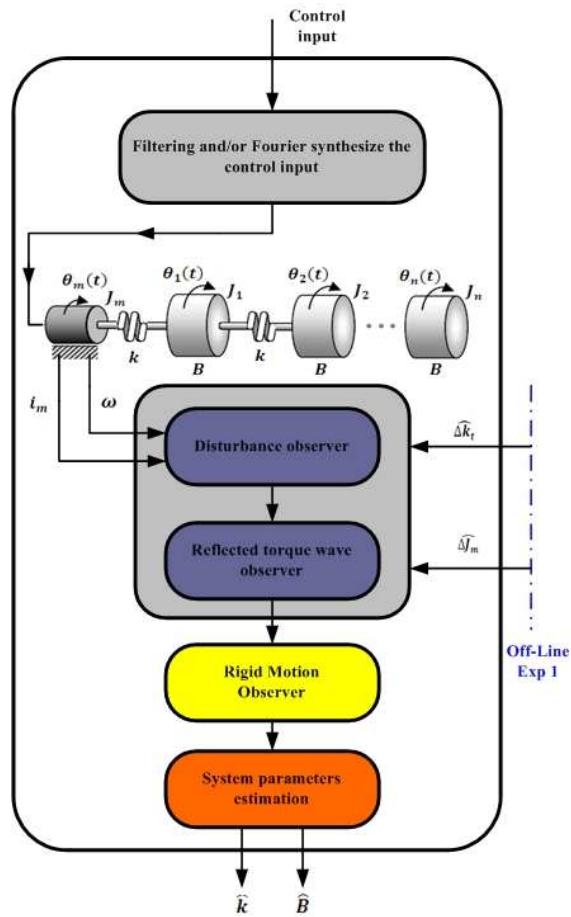
Figure 3.15: Off-line experiment 2

3.7.3 Sensorless control algorithm

The previous two off-line experiments are performed in order to estimate the motion of the flexible system and the externally applied disturbances due to its interaction with the environment. Figure.3.16 illustrates the sensorless motion and force control process that can be accomplished if the following procedures are followed:
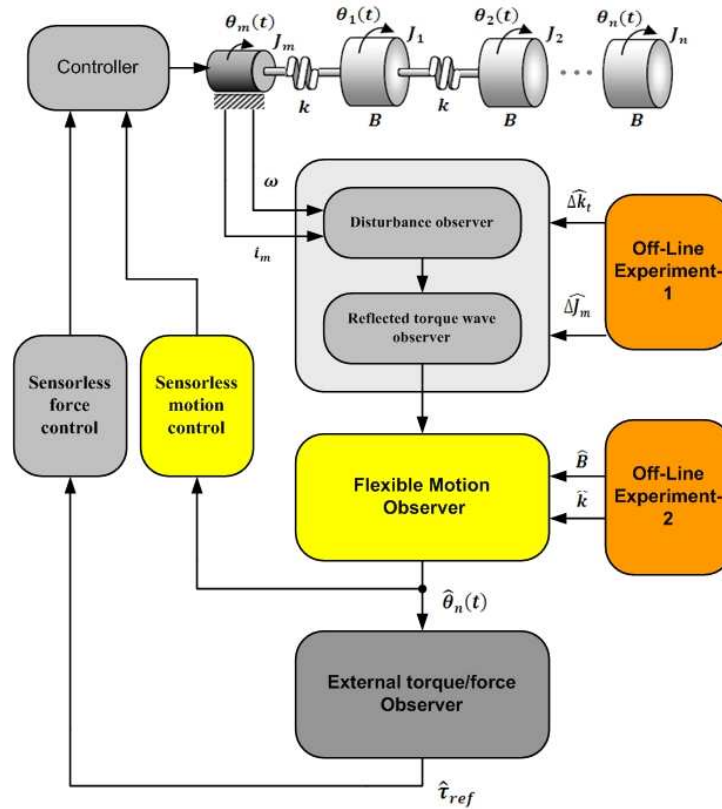
Figure 3.16: Sensorless motion/force control

1. Determining the varied self-inertia load's estimate and the torque ripple's estimate by performing off-line experiment 1.

2. Estimating the total disturbance $\widehat{d}$ using the actuator's current and velocity using Eq.3.13

3. Decoupling the reflected torque wave out of the total disturbance using Eq.3.30.

4. Constructing the flexible lumped masses motion's observers using the recursive Eq.3.49 along with the results obtained from off-line experiment 2.

5. Estimating the external torques or disturbances on the plant using Eq.3.51.

6. Feeding the position's estimates back to the controller to accomplish the sensorless motion and vibration control task.

7. Force control is also possible as the estimate of the external applied force or torque is available.

CHAPTER 4

Experimental Results

In order to investigate the validity of the proposed sensorless estimation algorithm, experiments are performed on a flexible system with three degrees of freedom as shown in Fig.4.1. The experimental setup consists of a direct drive DC motor connected to a lumped inertial system with three masses. The masses are connected to each other with similar springs. Each inertial mass is connected to an encoder in order to compare the estimated position with the actual measured one. Encoders are used to verify the performance of the positions's observers. The system is kept free from any measurements. Strictly speaking, the plant is kept free from any measurements but the actuator not as its current and velocity have to be measured for the subsequent analysis and estimations.

The following experiments are performed on the flexible system shown in Fig.4.1:

- Disturbance estimation-reflected torque estimation

- Rigid body motion estimation

- Uniform system's parameters estimation

- Flexible motion estimation

- Sensorless motion control

- Sensorless external torque estimation

Figure 4.1: Lumped inertial system

4.1 Disturbance Estimation

In order to extract the reflected torque out of the disturbance d, we have to estimate this disturbance first as it is used as an input for the second torque observer. Therefore, disturbance is estimated from the actuator's side using its current and velocity. Table.4.1 shows the experimental parameters of the disturbance estimation experiment.

Table 4.1: Experimental parameters-disturbance estimation

Disturbance estimation experiment			
Parameter	Value	Parameter	Value
k_{to}	40.6 mNm/A	J_{mo}	209 gcm^2
J_a	6192.707 gcm^2	g_{dist}	100 rad/sec

The obtained results are shown in Fig.4.2. The estimated disturbance is compared with the actual one in the simulation result shown in Fig.4.2.a, which indicates that

57
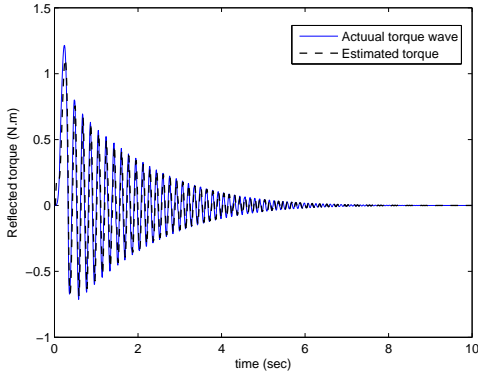
(a) Simulation of actual and estimated torque wave
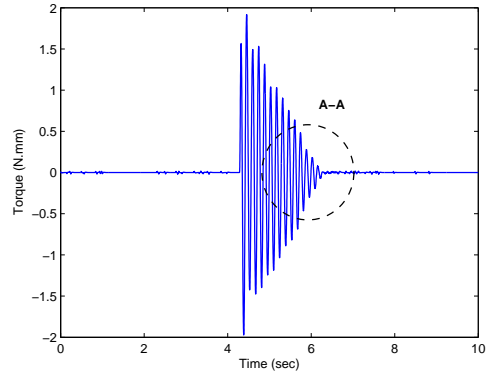
(b) Experimentally measured torque wave
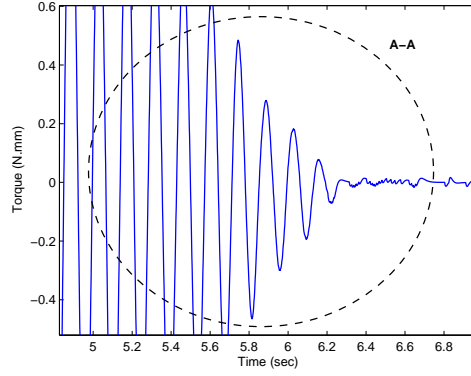
(c) Magnified plot of A-A

Figure 4.2: Reflected wave measurement

the estimated disturbance converges to the actual disturbance according to error's dynamics Eq.3.18. Figure.4.2.b shows the actual estimated disturbance when an inertial load is attached to the actuator. This disturbance is composed of the reflected load, the varied self-inertia torque and actuator's torque ripple. The last two terms can be eliminated in order to decouple the reflected torque $\widehat{\tau}_{ref}$ from the disturbance $\widehat{d}$ by performing off-line experiment-1 that enables the determination of actuator's parameter variation disturbance, then the reflected torque wave can be decoupled out of the total disturbance.

4.2 Rigid Body Motion Estimation

In order to estimate the uniform system's parameters, rigid motion has to be estimated first and then used in the parameters estimation equation Eq.3.39. The idea behind restricting the flexible system to rigidly move is the ability of describing the motion of the entire system with a single coordinate rather than n coordinates that is equal to the system's degrees-of-freedom. The rigid motion estimate is given by the following expression as it was proven in Chapter.3

$$\widehat{\theta}(t) = \frac{1}{\sum_{i=1}^{n} J_i} \int_o^t \int_o^t \widehat{\tau}_{ref} d\tau d\tau + c_1 t + c_2 \tag{4.1}$$

$$\widehat{x}(t) = \frac{1}{\sum_{i=1}^{n} m_i} \int_o^t \int_o^t \widehat{f}_{ref} d\tau d\tau + c_1 t + c_2 . \tag{4.2}$$

The last equations are valid in a narrow particular region of the system's frequency range. They are not valid at the system's resonance frequencies nor around them. Therefore, the control input has to be filtered to insure that the system's flexible modes will not be excited, or Fourier synthesized in order to insure that the control input is free from any energy at the system's resonance frequencies. Simply the control input has to satisfy Eq.3.34.

4.2.1 Experiment-1

The first rigid motion estimation experiment is performed on a 2 degrees of freedom inertial and linear system. The experimental parameters are summarized in Table.4.2.

Experiment-1 was performed on the system's low frequency range, below 5 rad/sec. The reason behind performing this experiment in this frequency range is to avoid exciting system's flexible modes, that will add more complicity to the computations. Eq.4.1 requires the reflected torque estimate[1]. Therefore, the reflected torque is estimated and used in Eq.4.1.

---

[1]The reflected torque was assumed to be equal to the total disturbance by the assuming that the reflected torque wave is much greater than the parameter's variation disturbance

Table 4.2: Experimental parameters-rigid motion estimation

Position estimation experiment		
Parameters	Inertial masses Exp	Linear masses Exp
J_1, m_1	6192.707 gcm^2	2641.8 g
J_2, m_2	200.17 gcm^2	2641.8 g
g_{dist}	100 rad/sec	100 rad/sec
Sampling time	1msec	1msec
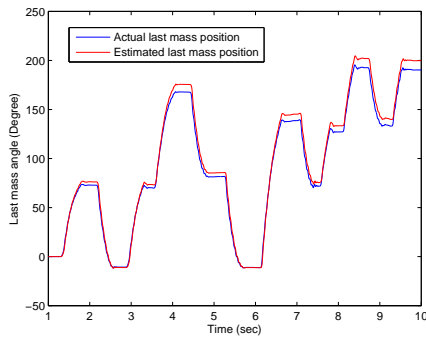
(a) Actual and estimated position
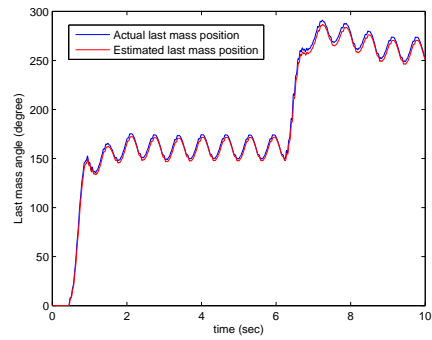
(b) Actual and estimated position
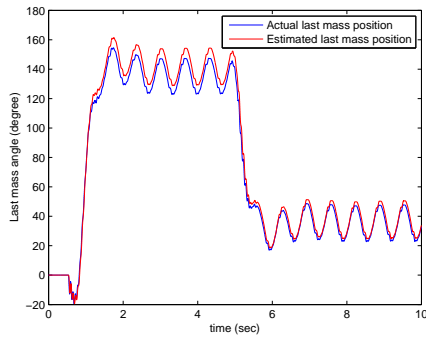
(c) Actual and estimated position
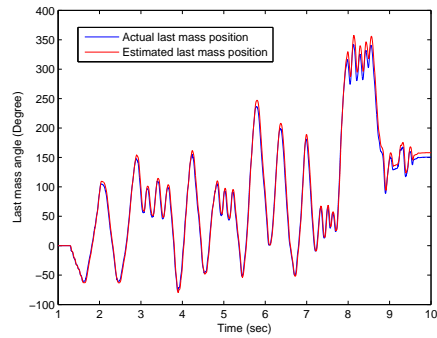
(d) Actual and estimated position

Figure 4.3: Experimental verification of position estimation
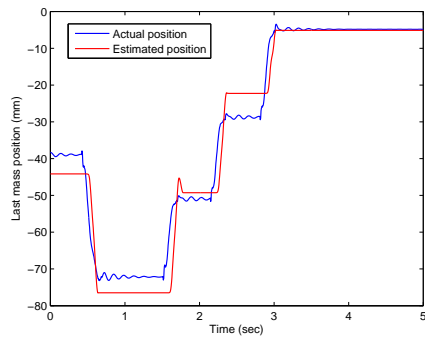
(a) Actual and estimated position
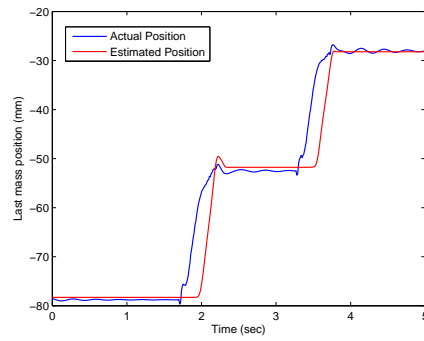
(b) Actual and estimated position
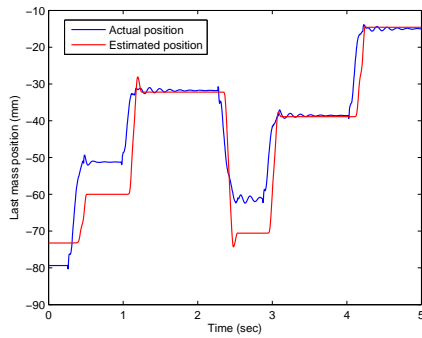
(c) Actual and estimated position
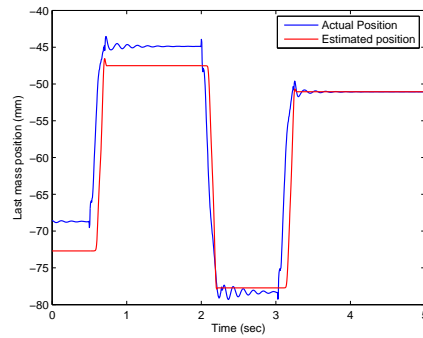
(d) Actual and estimated position

Figure 4.4: Experimental verification of position estimation

Fig.4.3 shows the estimated and actual position of the last mass of the inertial lumped system, while Fig.4.4 shows the last mass position's estimate and the actual encoder measurement for a lumped linear mass spring system. For both systems an arbitrary trajectory input is given to the system to examine the performance of the rigid motion observer by comparing the actual system's position with the estimated one.

The obtained results indicates that these equations can be used to provide an estimate for the rigid motion of the flexible system. Indeed, the double integration of the reflected torque wave signal will certainly amplify any initial error. Therefore, rigid motion estimation experiment[1] has to be performed for a short period of time.

---

[1]Since the mutidegree-of-freedom flexible modes are not excited by filtering the forcing function, only one encoder can be used to compare the actual system's rigid position with the estimated one.

The purpose is not to determine the rigid motion, its just a step in the parameters estimation process. Hence, the double integrators of Eq.4.1 and 4.2 will not represent any problems in this context.

4.2.2 Experiment-2

Table 4.3: Rigid body motion estimation-Experimental parameters

Parameter	Value	Parameter	Value
J_1	5152.99 gcm^2	J_3	6192.707 gcm^2
J_2	5152.99 gcm^2	f_1	1 rad/sec
f_2	2 rad/sec	f_3	3 rad/sec
f_4	4 rad/sec	f_5	5 rad/sec
g_{dist}	100 rad/sec	g_{lpf}	100 rad/sec

The second experiment was performed on a 3 degrees-of-freedom inertial system. The frequency of the arbitrary forcing function is varied in order to determine the frequency range at which the rigid motion estimation equations are valid. Table.4.3 summarizes the parameters of this experiment. The frequency of the forcing function was increased gradually between 0.5 rad/sec to 5 rad/sec. Fig.4.5 and 4.6 show the response[2] of the three lumped inertial masses and the estimate of the rigid motion at certain frequencies. It turns out that, at 3 rad/sec the estimated signal is no longer following the positions of the masses, and the masses them self are no longer behaving rigidly. Therefore, this particular flexible system is behaving rigidly below 3 rad/sec and the parameters estimation experiment has to be performed below this frequency.

---

[2]Since the forcing function's frequency is gradually increasing, system will no longer behave rigidly. Therefore, an encoder is attached to each mass to monitor their responses
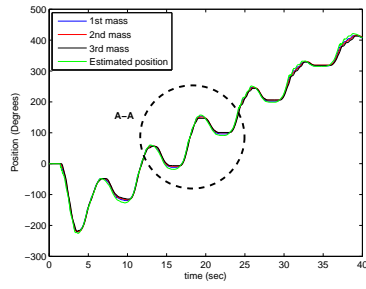
(a) $f_1 = 1$rad/sec
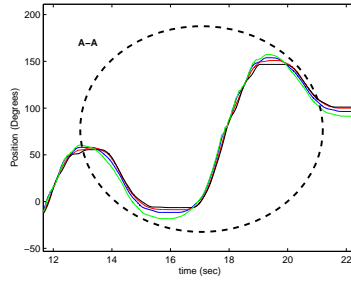
(b) Mag plot of a
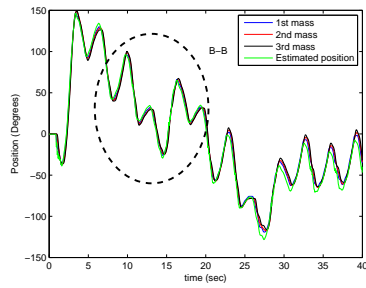
(c) $f_2 = 2$rad/sec
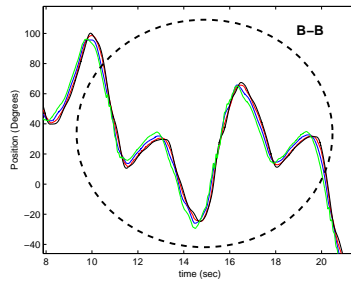
(d) Mag plot of c

Figure 4.5: Rigid body motion estimation
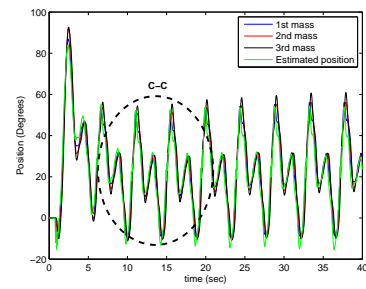
(a) $f_3 = 3$rad/sec
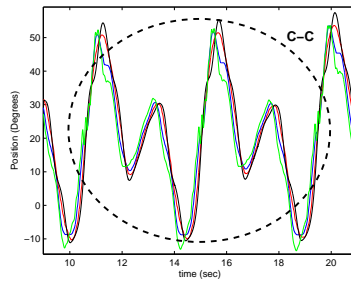
(b) Mag plot of a
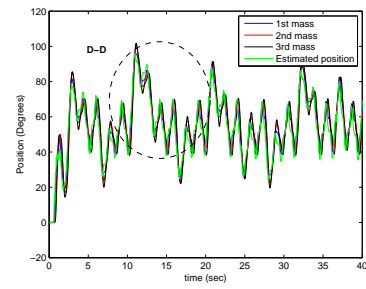
(c) $f_4 = 4$rad/sec
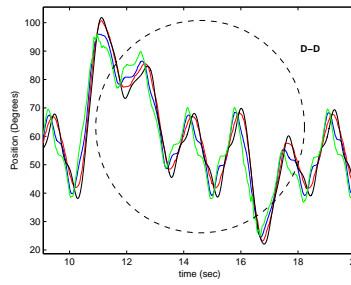
(d) Mag plot of c

Figure 4.6: Rigid body motion estimation

63

4.3 System's Uniform Parameters Estimation

The system's uniform parameters are estimated by the following equation

$$\begin{bmatrix} \widehat{k} \\ \widehat{B} \end{bmatrix} = \mathbf{G}^\dagger \begin{bmatrix} \widehat{\underline{\tau}}_{ref} \end{bmatrix} \tag{4.3}$$

where matrix $\mathbf{G}$ is obtained by concatenating two vectors, the first one is the difference between the actuator position data points and the rigid motion's estimation data points, the second vector is the derivative of the first one. The left hand side vector of Eq.4.3 is the solution that minimizes the norm square of errors. Table.4.4 shows the experimental parameters used in this experiment.

Table 4.4: Parameters estimation experiment

Parameter	Value	Parameter	Value
k_t	40.6 mNm/A	J_2	5152.99 gcm^2
J_m	209 gcm^2	τ(time const)	4.43 msec
k_b	235 rpm/v	g_{dist}	100 rad/sec
J_1	5152.99 gcm^2	Velocity LPF	100 rad/sec

The estimated stiffness and damping coefficients obtained using Eq.4.3 are included in Table.4.5 and 4.6. The average values for l experiments are computed as follows

$$\widehat{k}_{avg} = \frac{\sum_{i=1}^{l} k_i}{l} = \frac{\sum_{i=1}^{20} k_i}{20} = \frac{30.9306}{20} = 1.54653 \ kN/m \tag{4.4}$$

$$\widehat{B}_{avg} = \frac{\sum_{i=1}^{l} B_i}{l} = \frac{\sum_{i=1}^{20} B_i}{20} = \frac{1.6866}{20} = 0.08433 \ Nsec/m \ . \tag{4.5}$$

The value of the spring constant is known before hand by the following computation

$$K = \frac{Gd}{8c^3 n} \tag{4.6}$$

Table 4.5: Experimental parameters

Experiment	$\hat{K}$(kN/m)	$\hat{B}$ (Nsec/m)	Experiment	$\hat{K}$ (kN/m)	$\hat{B}$(Nsec/m)
1st Exp	1.5796	0.0888	6th Exp	1.5277	0.0892
2nd Exp	1.5336	0.0878	7th Exp	1.4913	0.0893
3rd Exp	1.6459	0.0887	8th Exp	1.5774	0.0892
4rd Exp	1.5116	0.0889	9th Exp	1.4531	0.0896
5rd Exp	1.5625	0.0893	10th Exp	1.6049	0.0891

where, G is the modulus of rigidity, d is the coil diameter, c is the spring index and n is the effective number of terns, Therefore, the system's uniform spring constant is

$$K = \frac{70 \times 10^9 \times 2}{8 \times (\frac{8}{2})^3 \times 21} = 1.627 \ kN/m \ .$$

Comparing the theoretical stiffness with the estimated one, we find that the difference is less than 5 percent. Despite of the small difference between the estimated and actual parameter, this difference will affect the subsequent computations and estimations. In other words, the recursive flexible motion equations depends on these estimated parameters. Therefore, a steady state error between the estimated positions and actual positions is expected.

Another way to examine whether the estimated parameters are close to the actual ones, is to reconstruct the reflected torque wave using the estimated parameters $\hat{k}$ and $\hat{B}$. Figure.4.7 shows the difference between the actual reflected torque wave and the reconstructed torque wave using the estimated uniform parameters. The reconstructed torque wave seems to have too much noise because of the direct differentiation that is used to reconstruct the wave. However, the reconstructed wave will not be used in any subsequent processes.

Table 4.6: Experimental parameters

Experiment	$\hat{K}$(kN/m)	$\hat{B}$ (Nsec/m)	Experiment	$\hat{K}$ (kN/m)	$\hat{B}$(Nsec/m)
1st Exp	1.4285	0.0895	6th Exp	1.6445	0.0886
2nd Exp	1.6540	0.0888	7th Exp	1.5051	0.0888
3rd Exp	1.4520	0.0883	8th Exp	1.6070	0.0882
4rd Exp	1.6321	0.0881	9th Exp	1.4972	0.0884
5rd Exp	1.4663	0.0884	10th Exp	1.5563	0.0880

(a) $\hat{k} = 1.579$ $\hat{B} = 0.088$ (b) $\hat{k} = 1.533$ $\hat{B} = 0.087$ (c) $\hat{k} = 1.654$ $\hat{B} = 0.088$

(d) Magnified Plot A-A   (e) Magnified Plot B-B   (f) Magnified Plot C-C
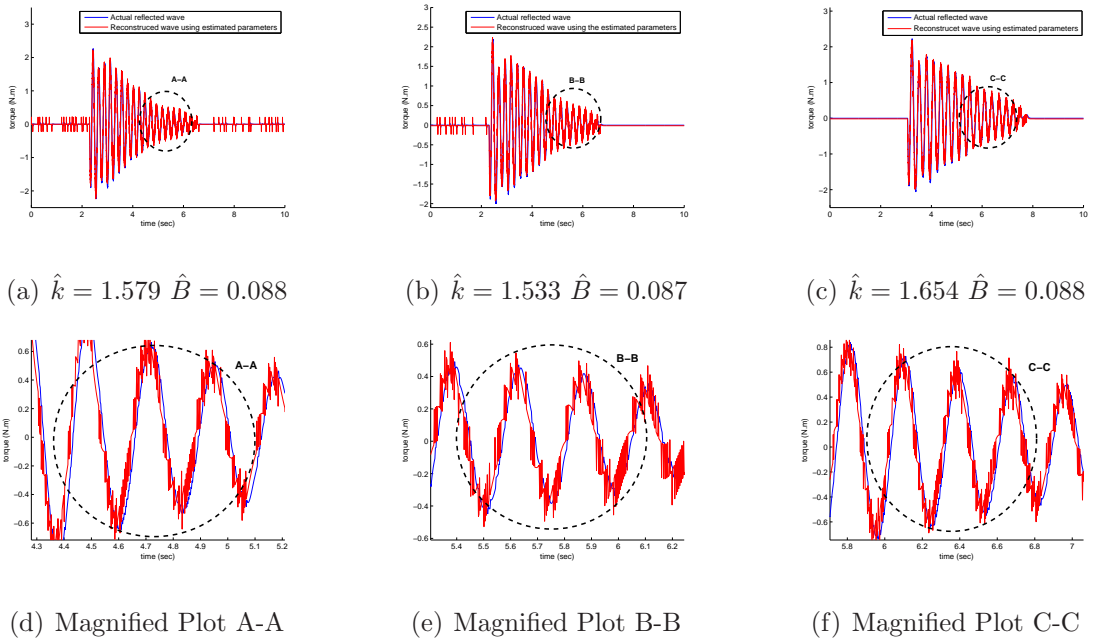
Figure 4.7: Estimated torque and reconstructed torque using estimated parameters

4.4 Flexible Motion Estimation

The recursive equations derived in Chapter.3 can be used in order to estimate the position of each lumped mass individually, regardless to the frequency of the forcing function, and regardless to the frequency content of the control input. Therefore, the recursive equations that estimate system's flexible motion provides us with a global behavior of the flexible system through its entire frequency range. Figure.4.8 shows the flexible behavior of a 3 degrees-of-freedom system when the control input excites

66

its flexible modes. In order to estimate each individual mass's position we use the following recursive equations

$$\widehat{\theta}_i(t) = e^{-\frac{\widehat{k}}{\widehat{B}}t} \int_o^t \Omega \; e^{\frac{\widehat{k}}{\widehat{B}}\tau} d\tau + e^{-\frac{\widehat{B}}{\widehat{k}}t} c_i \tag{4.7}$$

$$\Omega \triangleq \frac{\Psi}{\widehat{B}}$$

$$\Psi \triangleq g(J_{i-1}, \widehat{\theta}_{i-1}, \widehat{\dot{\theta}}_{i-1}, \widehat{\ddot{\theta}}_{i-1}, \widehat{k}, \widehat{B}) \; .$$
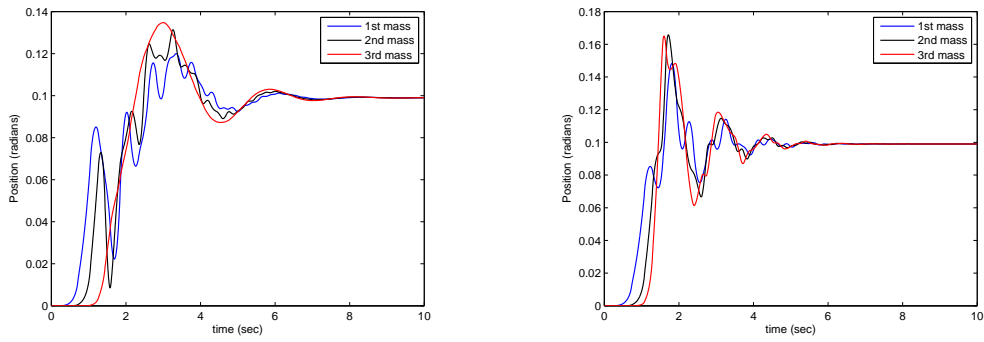
Figure 4.8: Flexible oscillation of a 3DOF dynamical dystem
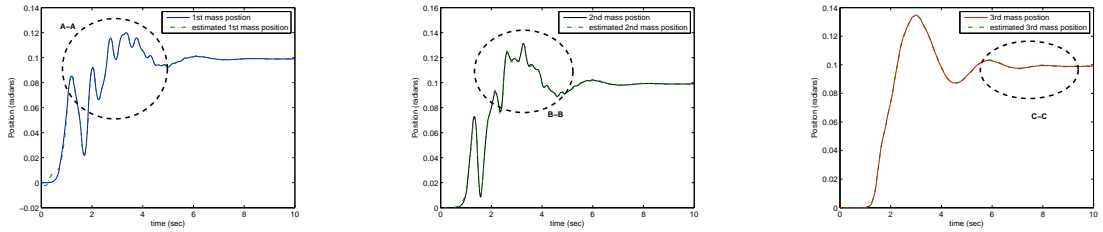
(a) 1st Mass and Its Estimate

(b) 2nd Mass and Its Estimate

(c) 3rd Mass and Its Estimate
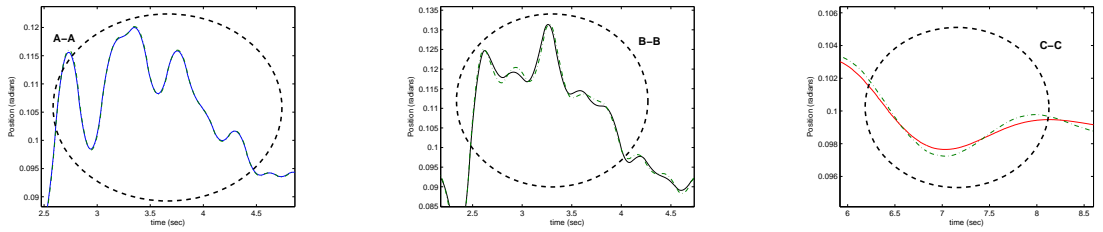
(d) Magnified Plot A-A

(e) Magnified Plot B-B

(f) Magnified Plot C-C

Figure 4.9: Flexible body motion estimation experimental results
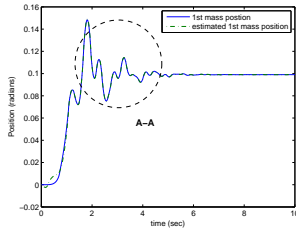
(a) 1st Mass and Its Estimate   (b) 2nd Mass and Its Estimate   (c) 3rd Mass and Its Estimate
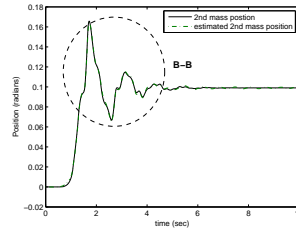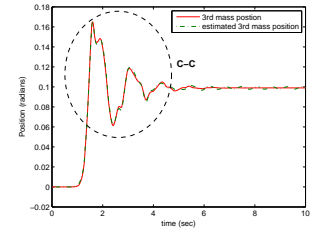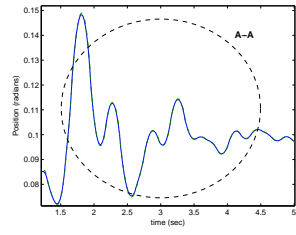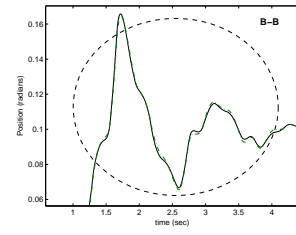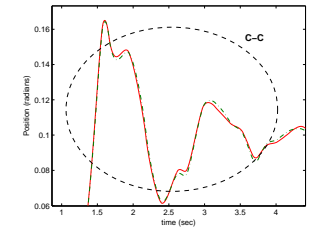
(d) Magnified Plot A-A   (e) Magnified Plot B-B   (f) Magnified Plot C-C

Figure 4.10: Flexible body motion estimation experimental results

The implementation of the recursive flexible motion equations requires performing all the previous experiments, since the parameters estimates $\widehat{k}$ and $\widehat{B}$ are required along with the estimated reflected torque wave $\widehat{\tau}_{ref}$.

Figure.4.9 shows the difference between the actual lumped masses' positions and the estimated positions for the flexible oscillations in Fig.4.8-a while the estimated positions of the flexible oscillations in Fig.4.8-b are shown in Fig.4.10. It turns out that the estimated positions are too close to the actual measurement taken by the encoders. Therefore, estimating the flexible motion for each lumped mass of the flexible system makes it possible to use these estimates instead of the actual measurements to construct a sensorless feedback control system.

4.5   External torque estimation

Estimation of the external disturbances on the flexible system requires the determination of the system's dynamics along with the estimate of the reflected torque wave,

68

using Eq.3.51. In this experiment, externally applied torque is applied by attaching another actuator to any of system's the lumped inertial masses. The actual external applied torque was measured using the actuator current and its torque constant as follows

$$\tau_{ext} = i_{ext} k_{ext} \tag{4.8}$$
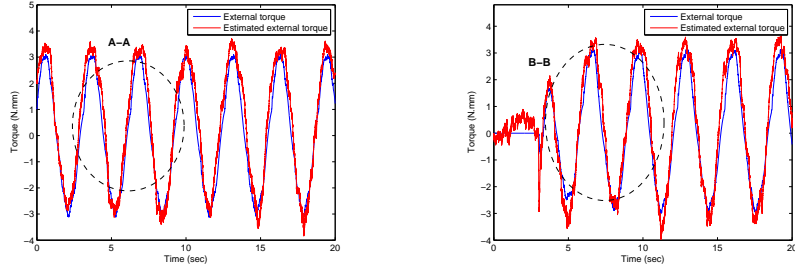
(a) estimated and external torque

(b) estimated and external torque
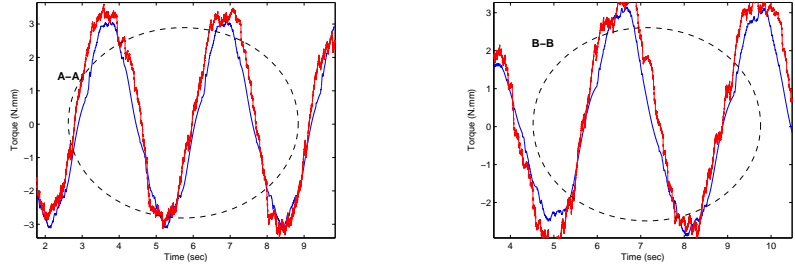
(c) Magnified plot of A-A

(d) Magnified Plot B-B

Figure 4.11: External torque estimation-$\tau_{ext} \mid_{f=2rad/sec}$

where τ_{ext} is the externally applied torque as an external disturbance and required to be estimated, i_{ext} and k_{ext} are the second actuator's current and torque constant. Therefore, the externally applied torque is known beforehand and its estimate can be computed by the following estimation based equation

$$\widehat{\tau}_{ext} = \sum_{i=1}^{n} J_i \widehat{\ddot{\theta}}_i - \widehat{\tau_{ref}} \tag{4.9}$$

which indicates that externally applied torques can be estimated if we obtain the system dynamics estimates and the reflected torque wave. That in turn requires es-
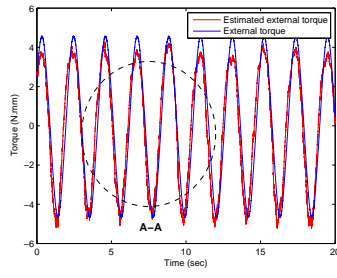
(a) estimated and external torque
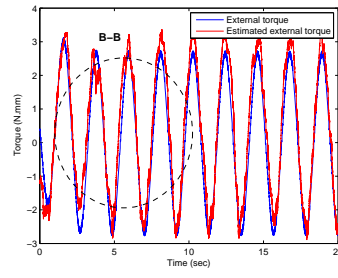
(b) estimated and external torque
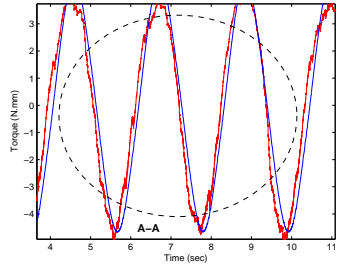
(c) Magnified plot of A-A
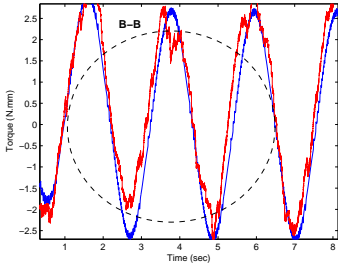
(d) Magnified Plot B-B

Figure 4.12: External torque estimation-$\tau_{ext}\mid_{f=4rad/sec}$

timating the system's flexible motion and estimating system parameters. In other words, in order to estimate the externally applied disturbances we have to go through the entire proposed algorithm along with performing all the related off-line experiments.

Figure.4.11 shows the difference between the actual and estimated externally applied torque. For a sinusoidal torque disturbance with frequency 2 rad/sec. Fig.4.12 shows the same result when the frequency of the sinusoidal disturbance is increased to 4 rad/sec.

4.6 Sensorless Motion control

4.6.1 Set-Point tracking experiment

In order to control the position of any lumped mass of the flexible system, measurements have to be taken from the point to be controlled. Consequently, position

70

sensors have to be attached to the points of interest. In our case, we have an estimate for each lumped mass position, that enables us to control any mass of the flexible system without attaching multiple sensors or changing their positions. All what we have to do is to feed the proper estimate back to the controller.

In the following experiment a 3 degrees-of-freedom system is used. Some of the position estimates can be used as a feedback when its required to control certain point of interest, while the other estimates can be used for monitoring some other features such as the residual vibrations in the flexible system.

Sensorless control of the 1st mass
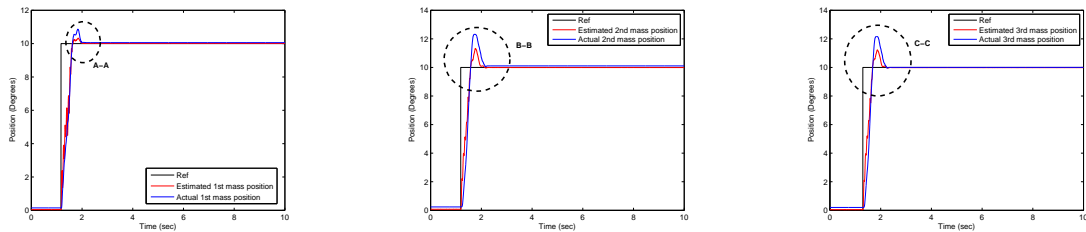
(a) Controlled 1st mass $k_p =$ 0.06 $k_d = 0.002$

(b) 2nd mass and its estimate

(c) 3rd mass and its estimate
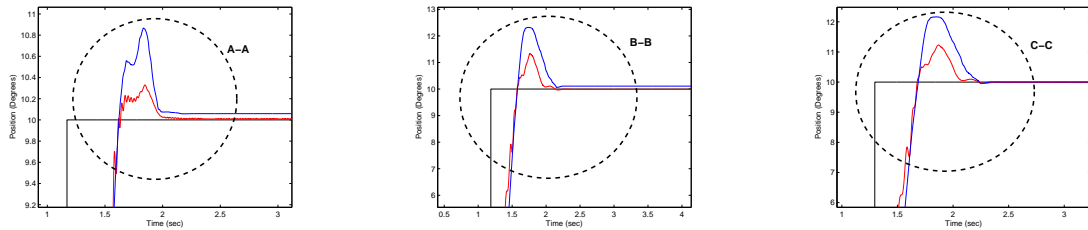
(d) Magnified plot A-A

(e) Magnified plot B-B

(f) Magnified plot C-C

Figure 4.13: Sensorless motion control experimental results (1st lumped mass estimate fed Back to the controller)

Figure.4.13 shows the sensorless control results of the first mass of the lumped system, where the estimate of the first mass position is fed back to the controller and the following control law is used

$$u(t) = k_p(\theta_{ref} - \widehat{\theta}_1) + k_d(\dot{\theta}_{ref} - \widehat{\dot{\theta}}_1) \; . \tag{4.10}$$

The estimation based PD control law seems to be satisfactory and different transient responses can be obtained by changing the controller gains. But the main problem is the steady state error that exists in the final response, which limits the accuracy of the controller. this steady state error depends on the accuracy of the estimators and observers that are used in the controller.

Sensorless control of the 2nd mass

Controlling the second mass requires feeding its position estimate back to the controller, the following PD control law is used

$$u(t) = k_p(\theta_{ref} - \widehat{\theta}_2) + k_d(\dot{\theta}_{ref} - \widehat{\dot{\theta}}_2) \; . \tag{4.11}$$

Fig.4.14 shows the global behavior of the lumped flexible system, where the second mass is controlled and positioned to a reference position. Other estimates can be used to ensure that system is free from residual vibrations. In other words, at the end controlled mass's travel, system has to be free from any kinetic and potential energies within its energy storage elements.

Sensorless control of the 3rd mass

Similarly, the third mass is controlled by the following control law.

$$u(t) = k_p(\theta_{ref} - \widehat{\theta}_3) + k_d(\dot{\theta}_{ref} - \widehat{\dot{\theta}}_3) \; . \tag{4.12}$$

Indeed, feeding the last mass position or its estimate to the controller turns the system into non-collocated control system that is hard to be controlled compared with the collocated control systems at which there exist no energy storage elements between the sensor and the actuator.
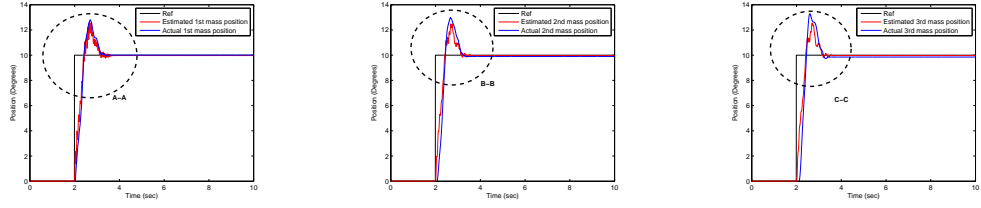
(a) 1st mass and its esti-
mate

(b) Controlled 2nd mass
$k_p = 0.002$ $k_d = 0$

(c) 3rd mass and its esti-
mate
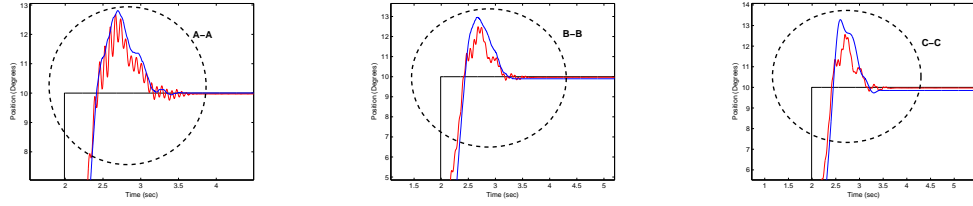
(d) Magnified plot A-A

(e) Magnified plot B-B

(f) Magnified plot C-C

Figure 4.14: Sensorless motion control experimental results (2nd lumped mass esti-
mate fed back to the controller)

Figure.4.15.c shows the response of the controlled last mass while Fig.4.15.a and
Fig.4.15.b show the behavior of the first and second masses respectively. The oscil-
latory behavior of the last mass is due to the non-collocated nature of the system.
In other words, shifting the virtual sensor to the last mass or feeding the last mass
position estimate to the controller results in a transfer function with no zeros. Which
in turn implies that shifting the virtual sensor along the flexible system results in
zeros immigration along or near the imaginary axis. Moreover, as the virtual sensor
is shifted away from the actuator, zeros move toward infinity in the complex plane.
Therefore, ending up with a non-collocated transfer function with no zeros. Since
system's zeros are frequencies at which system has zero outputs for non-zero inputs,
zeros are considered to stabilize the system. Eventually, the oscillatory behavior of
the controlled last mass shown in Fig.4.15.c is due to the existence of energy storage
elements between the actuator and the sensor without having frequencies (zeros) at
which this energy can be attenuated.
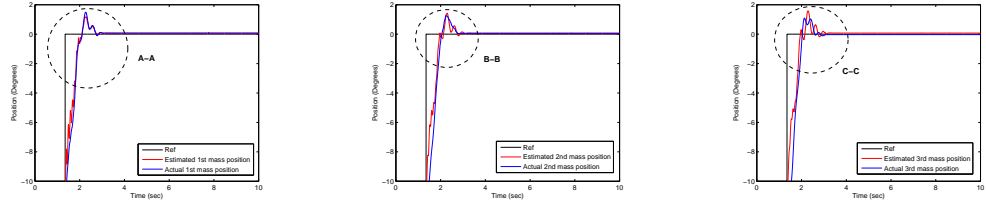
(a) 1st mass and its esti-
mate

(b) 2nd mass and its esti-
mate

(c) Controlled 3rd mass
$k_p = 0.008$ $k_d = 0.09$
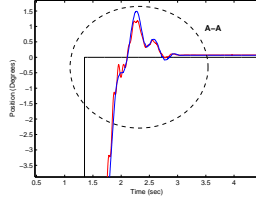
(d) Magnified plot A-A
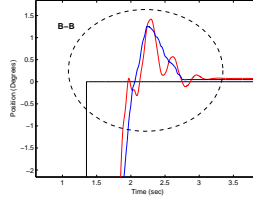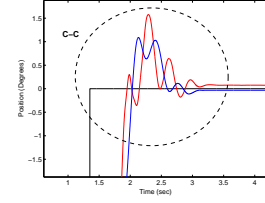
(e) Magnified plot B-B

(f) Magnified plot C-C

Figure 4.15: Sensorless motion control experimental results (3rd lumped mass estimate
fed back to the controller)

4.6.2 Sensorless trajectory tracking

Instead of just using a reference input, a timing varying trajectory[3] can be used as
the reference that is required to be tracked. Figure.4.16 shows the results of the
trajectory tracking experiments, where a square and sawtooth signals are used as
a reference trajectory. In this experiment the last mass was following the reference
trajectory using an estimation based PD controller. Indeed, the trajectory tracking
requires a feed forward term to be added to the control signal. But the results shown
in Fig.4.16 are obtained with just the estimation PD control law Eq.4.12.

The feed forward control terms requires the determination or the knowledge of the
system dynamics and parameters. Therefore, this sensorless estimation algorithm
makes it possible to achieve the feed forward control problem and the trajectory

---

[3]In order to follow a time varying trajectory, an additional feed forward control input has to
be added to the control input. The feed forward control input can be computed as the system's
dynamics estimates are available
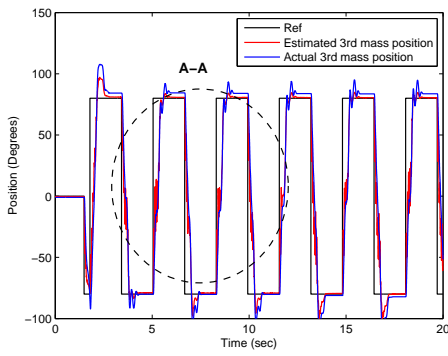
(a) Estimated, actual and reference square trajectory $k_p = 0.06 - k_d = 0.0025$
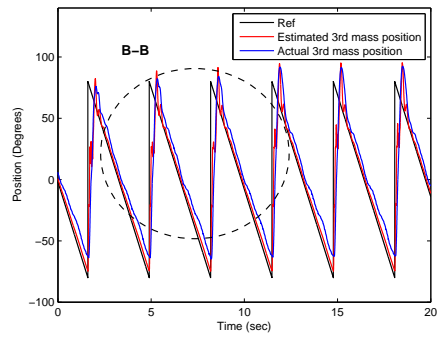
(b) Estimated, actual and reference triangular trajectory $k_p = 0.09 - k_d = 0.004$
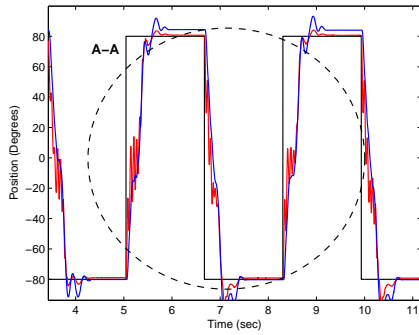
(c) Magnified plot of A-A
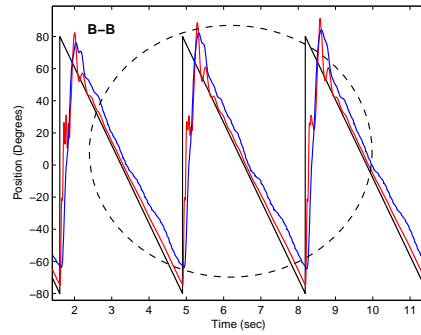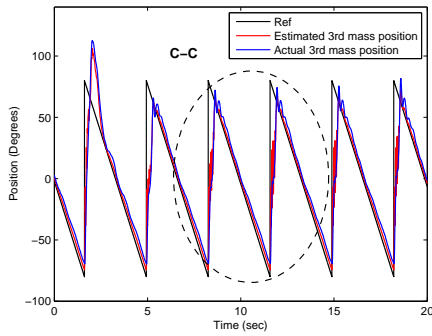
(d) Magnified Plot B-B

(e) Estimated, actual and reference square trajectory $k_p = 0.1 - k_d = 0.0042$
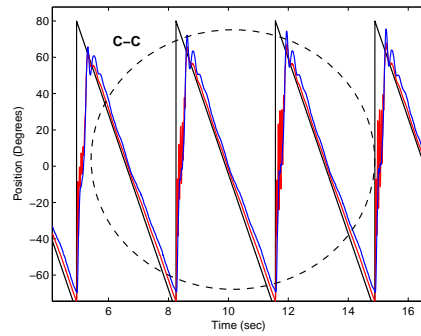
(f) Magnified Plot B-B

Figure 4.16: Trajectory tracking experiment-third mass

tracking control in a sensorless manner without attaching any sensors to the flexible system.

CHAPTER 5

Conclusions

In this thesis, a sensorless motion control is presented and experimentally evaluated on a multi degrees-of-freedom flexible system. The obtained results show the possibility of using the actuator as a single platform for measurement, estimation and control keeping the flexible system free from any attached sensors. Considering the reflected mechanical waves from the system to the actuator as a natural feedback that contains enough information about system's dynamics, parameters and external disturbances.

The reflected waves are investigated in order to prove that they contain these information. In addition, the wave's propagation behavior is also investigated in order to prove the possibility of measuring or estimating such waves from the actuator side to keep the plant free from measurement.

Disturbance observer's structure is modified in order to decouple the reflected mechanical waves out of the total disturbance on the actuator. Then, the sensorless estimation algorithm is introduced based on measuring current and velocity from the actuator side and estimate of the reflected mechanical wave from the plant side. The proposed algorithm makes it possible to observe the rigid motion of the flexible system, to estimate system's uniform parameters, observe each individual mass's flexible motion and to estimate any external disturbances added to the plant due to any interaction with the environment. Therefore, sensorless motion control of flexible dynamical system can be accomplished using two measurements from the actuator. Moreover, each lumped mass of the flexible system can be controlled and the rest of

the system can be monitored in a sensorless manner. Hence, motion control of flexible system can be accomplished along with reducing the residual vibrations that can be monitored without measurements.

Indeed, extracting all of these information out of few measurements from the actuator is not possible unless two off-line experiments are performed. Firstly, the varied self-inertia torque and actuator's torque ripple are estimated experimentally and then used to modify the structure of the conventional disturbance observer. The new disturbance observer's configuration introduced in this thesis makes it possible to decouple the disturbances terms. Secondly, the system uniform parameters are estimated with another off-line experiment. The estimated system parameters are compared to the actual theoretical ones that are known beforehand and the difference between the estimated and theoretical values is less than 5 percent that can be acceptable for certain applications such as vibration control and motion control problems that do not require very accurate positioning.

The proposed algorithm is also based on the different behavior of the flexible system through the entire system's frequency range. Which makes it possible to estimate the uniform system parameters and to use them in the general recursive equations that describe the system's flexible motion through the entire system's frequency range.

Sensorless motion control experiments show that it is easier to use the estimate of the lumped masses positions than using multiple sensors or changing their locations to control certain point of interest if the actual measurements are used. Accuracy of the motion control process depends on the accuracy of the flexible motion observers, parameters estimators and the off-line experiments. Therefore, steady state error exists in the final response. This steady state error can be minimized by performing some operational enhancement and more accurate off-line experiments.

In this thesis flexibility is not considered as problem to be avoided, wave reflections are not considered as disturbance that have to be rejected. Instead, disturbance and

flexibility are considered as the core of a sensorless estimation process that deals with the disturbance as a coupled signals that are rich with enough information about the dynamical system and with the flexibility as a tool to decouple each single piece of information out of this disturbance. Eventually, we can conclude that:

- Mechanical waves can be considered as a natural feedback from flexible system.

- Disturbance on the actuator side carries information about system parameters, dynamics and externally applied torques/forces due to system interaction with the environment.

- Disturbance observer can be modified to provide two outputs used to achieve both robust and sensorless motion control.

- Flexibility of the system can be used as a tool to decouple the required information from the reflected mechanical wave.

- Actuator can be used as a single platform to perform the necessary estimations required to control flexible systems.

- Motion, vibration and force control can be accomplished without attaching any sensor to the flexible system.

5.1   Future Work

Distributed flexible systems such as flexible robot arms, beams and manipulators require special sensors with certain specifications to accomplish feedback control. Stain gages have to be flexible enough to withstand the fatigue stresses imposed due to the everlasting fluctuations of these systems. Moreover, the inaccurate kinematic mapping between the point at which measurements are taken and point to be controlled causes steady state error in the final response. On the other hand, visual feedback

requires certain environmental setup with proper illumination to ensure reliable results. In other words, due to the flexibility and the distributed nature of these systems attaching a sensor or obtaining a reliable feedback seems to be hard.

Therefore, considering reflected mechanical waves as a natural feedback from these distributed system makes it possible to keep them free from any attached sensors and the sensorless estimation algorithm can be implemented on these distributed systems. Indeed, the previous analysis are performed on lumped flexible system and so do the experiments but distributed systems can also be approximated by finite number of masses along with a low pass filter can to attenuate the residual mode spill-over effects. Therefore, as a future work the proposed algorithm can be implemented on distributed flexible systems such as flexible robot arms, beams and manipulators.

BIBLIOGRAPHY

[1] W. J. O'Connar, "Wave-based analysis and control of lump-modeled flexible robots," in *Proc. IEEE Transaction on robotics'07*, vol. 23, pp. 342–352, Apr. 2007.

[2] W. J. O'Connar, "Control of flexible mechanical systems:wave-based techniques," in *Proc. American Control Conference'07*, vol. 1, (New York, NY), pp. 4192–4202, July 2007.

[3] W. J. O'Connar, "Wave-echo position control of flexible systems: Toward an explanation and theory," in *Proc. AACC American Control Conference'04*, vol. 1, (Boston, Massachusetts), pp. 4837–4842, July 2004.

[4] W. J. O'Connar, "Wave-based control of flexible mechanical systems," in *Proc. TOK Automatic Control Conference'07*, vol. 1, (Istanbul), pp. 1–5, June 2007.

[5] W. J. O'Connar, "A gantry crane problem solved," in *Proc. ASME Journal of ynamic System, Measurement, and Control'03*, vol. 125, pp. 569–576, Dec. 2003.

[6] W. J. O'Connar, "Wave-echo control of lumped flexible systems," in *Proc. ScienceDirect '06*, vol. 298, pp. 1001–1018, June 2006.

[7] D. J. Mckeown and W. J. O'Connar, "Wave-based control-implementation and comparisons," in *Proc. American Control Conference'07*, vol. 1, (New York, NY), pp. 4209–4214, July 2007.

[8] F. Ramos and W. J. O'Connar, "Non-linear behavior in wave-based control," in

Proc. American Control Conference'07, vol. 1, (New York, NY), pp. 4203–4208, July 2007.

[9] M. Sugita, T. Murakami, and K. Ohnishi, "Following control of flexible manipulator," in *Proc. IEEE International Control for Intelligent Automation'92*, vol. 1, (Italy), pp. 367–372, Oct. 1992.

[10] K. Ohnishi, M. Shibata, and T. Murakami, "Motion control for advanced mechatronics," in *Proc. IEEE/ASME Transaction On Mechatronics'96*, vol. 1, pp. 56–67, Mar. 1996.

[11] T. Murakami and K. Ohnishi, "Observer-based motion control-application to robust control and parameters identification," in *Proc. IEEE '93*, vol. 1, pp. 1–6, June 1993.

[12] T. Tsuji, M. Mizuochi, H. Nishi, and K. Ohnisi, "A velocity measurement method for acceleration control," in *Proc. IEEE '05*, vol. 1, pp. 1943–1947, Mar. 2005.

[13] T. Murakami, F. Yu, and K. Ohnishi, "Torque sensorless control in multidegreee-of-freedom manipulator," in *Proc. IEEE Transaction On Industrial Electronics'07*, vol. 40, pp. 259–265, Apr. 1993.

[14] T. Murakami and K. Ohnishi, "Robust and adaptive control strategies," in *Proc. IFAC International Control for Intelligent Automation'92*, vol. 1, (Italy), pp. 367–372, Oct. 1992.

[15] S. Katsura and K. Ohnishi, "Force servoing by flexible manipulator based on resonance ration control," in *Proc. IEEE Transaction On Industrial Electronics'07*, vol. 54, pp. 539–547, Feb. 2007.

[16] E. Schrijer, J. V. Dijk, and H. Nijmeijer, "Equivalence of disturbance observer

structure for linear systems," in *Proc. IEEE Conference on Decision and Control'00*, vol. 54, (Sydney, Australia), pp. 4518–4519, Dec. 2000.

[17] S. P. Bhat and M. D. K, "Solutions to point-to-point control problems using laplace transform technique," in *Proc. ASME Journal of Dynamic Systems, Measurement And Control'91*, vol. 113-3, pp. 425–431, Sept. 1991a.

[18] S. P. Bhat and M. D. K, "Experimentats on point-to-point position control of flexible beam using laplace transform technique," in *Proc. ASME Journal of Dynamic Systems, Measurement And Control'91*, vol. 113-3, pp. 438–443, Sept. 1991c.

[19] S. P. Bhat and M. D. K, "Precise point-to-point positioning control of flexible structures," in *Proc. ASME Journal of Dynamic Systems, Measurement And Control'90*, vol. 112-4, pp. 667–674, Dec. 1990.

[20] S. Sugiyama and K. Uchino, "Pulse driving methode of piezoelectric motors," in *IEEE Journal'86*, pp. 637–640, Dec. 1986.

[21] D. M. Aspinwall, "Acceleration profile for minimizing residual response," in *Proc. ASME Journal of Dynamic Systems, Measurement And Control'80*, vol. 102-2, pp. 3–6, May 1980.

[22] P. Meckl and W. Seering, "Reducing residual vibration in systems with time-varying resonances," in *Proc. International Conference on Robotics and Automation'87*, pp. 1690–1695, Dec. 1986.

[23] D. K. Miu, *Mechatronics*, pp. 157–159. Springer-Verlag, 1st ed., 1993.

[24] W. A. Strauss, *Partial Differnetial Equations-An Introduction*, pp. 32–52. John Wiley, ninetheeth ed., 1992.

[25] H. Ojima, K. Nagase, and Y. Hayakawa, "Wave-based analysis and wave control of damped mass-spring systems," in *Proc. IEEE Conference on Decision and Control'01*, vol. 1, (Orlando, Florida), pp. 2574–2579, Dec. 2001.

[26] F. M. Aldebrez, M. O. Tokhi, Z. Mohamed, and S. M. Ahmad, "Vibration control of pitch movement using command shaping techniques," in *Proc. IEEE The Transaction of Electrical And Electronics Engineers'03*, vol. 1.

[27] Korimoto and Kagoshima, "Robot motion control based on joint torque sensing," in *Proc. IEEE '89*, vol. 1, pp. 256–261, Mar. 1989.

[28] J. W. L. Simpson, C. D. Cook, and Z. Li, "Sensorless force estimation for robots with friction," in *Proc. ARAA Australasian Conference in Robotics and Automation'02*, vol. 1, (Auckland,), pp. 94–99, Nov. 2002.

[29] O. Hirayama, K. Ohtsuka, S. Ishiwata, and S. Watanabe, "Nonlinear waves in mass-spring systems with velocity-dependent friction," in *Proc. ScienceDirect'03*, pp. 97–116, June 2003.

[30] K. Matsuda, Y. Kanemitsu, and S. Kijimoto, "A wave-based controller design for general flexible structures," in *Proc. Jouranl of Sound and Vibration'98*, vol. 1, pp. 269–279, Mar. 1998.

[31] J. Cheong, W.-K. Chung, Y. Youm, and S. rok Oh, "Control of two-link flexible manipulator using disturbance observer with reaction torque feedback," in *Proc. IEEE ICAR'97*, vol. 1, pp. 227–232, July 1997.

[32] yoichi Hori, H. Sawada, and Y. Chun, "Slow resonance ration control for vibration suppression and disrutbance rejection in torisional system," in *Proc. IEEE Transaction on Industrial Electronics'99*, vol. 46, pp. 162–168, Feb. 1999.

[33] M. Isogai, F. Arai, and T. Fukuda, "Modeling and vibration control with neural network for flexible multi-link structures," in *Proc. IEEE Internaltional Conference on Robotics and Automation'99*, (Detroit, Michigan), pp. 1096–1101, May 1999.

[34] M. J. Balas, "Active control of flexible systems," in *Proc. Journal Of Optimization theory and Application'78*, vol. 25, (Blacksburg, Virginia), pp. 415–436, July 1978.

[35] M. C. Tsai, E. C. Tseng, and M. Y. Cheng, "Design of a torque observer for detecting abnormal load," in *Proc. Control Engineering Practice'00*, vol. 8, pp. 259–269, Aug. 2000.

[36] C. L. Lin and V. T. Liu, "Robust active control of flexible systems with structured perturbations," in *Proc. IEEE Conference on Decision and Control'92*, vol. 1, (Yucson, Arizona), pp. 2432–2435, Dec. 1992.

[37] B. Bandyupadhyay and A. J. Mehta, "vibration control of smart structure using second order sliding mode control," in *Proc. IEEE Conference on Control Applications'05*, vol. 1, (Toronto, Canada), pp. 1691–1696, Aug. 2005.

[38] M. Rodic and K. Jezernik, "Speed-sensorless sliding-mode torque control of an induction motor," in *Proc. IEEE Transaction on Industrial Electronics'02*, vol. 49, pp. 87–95, Feb. 2002.

[39] W. Reinelt, "Robust control of a two-mass-spring system subject to its input constraints," in *Proc. AACC American Control Conference'00*, (Chicago, Illinois), pp. 1817–1821, June 2000.

[40] Y. Ohba, S. Katsura, and K. Ohishi, "Sensorless force control for machine tool using reaction torque observer," in *Proc. IEEE '06*.

[41] H. Kobayashi, S. Katsura, and K. Ohnishi, "An analysis of parameter variation of disturbance observer for motion control," in *Proc. IEEE Transaction On Industrial Electronics'07*, vol. 54, pp. 3413–3421, Dec. 2007.

[42] S. Katsura, Y. Matsumoto, and K. ohnishi, "Modeling of force sensing and validation of disturbance observer for force control," in *Proc. IEEE Transaction On Industrial Electronics'07*, vol. 54, pp. 530–538, Feb. 2007.

[43] S. Katsura, Y. Matsumoto, and K. ohnishi, "Realization of law of action and reaction by multilateral control," in *Proc. IEEE Transaction On Industrial Electronics'05*, vol. 52, pp. 1196–1205, Oct. 2005.

[44] W. H. Zhu, Z. Bien, and J. D. Schutter, "Adaptive motion/force control of multiple manipulator with joint flexibility based on virtual decomposition," *IEEE Transaction On Automatic Control*, vol. 43, pp. 46–50, Jan 1998.

[45] Y. Huang and W. Messner, "A novel disturbance observer design for magnetic hard drive servo system with a rotary actuator," *IEEE Transaction On Magnetics*, vol. 34, pp. 1892–1894, Jull 1998.

APPENDIX A

Solution of The Wave Equation

The one dimensional wave equation is described by the following partial differential equation

$$\frac{\partial^2 u(x,t)}{\partial t^2} - c^2 \frac{\partial^2 u(x,t)}{\partial x^2} = H(t,x) \ . \tag{A.1}$$

Solution of this equation is decomposed of both natural and forced response, by the super-position principle we can separate the non-homogenous wave equation into two problems

$$\frac{\partial^2 v(x,t)}{\partial t^2} - c^2 \frac{\partial^2 v(x,t)}{\partial x^2} = 0 \tag{A.2}$$

and

$$\frac{\partial^2 w(x,t)}{\partial t^2} - c^2 \frac{\partial^2 w(x,t)}{\partial x^2} = H(t,x) \tag{A.3}$$

by solving the homogenous one dimensional wave equation eq.A.2 , which is nothing but two transport equations and could be represented as follow

$$(\frac{\partial}{\partial t} - c\frac{\partial}{\partial x})(\frac{\partial}{\partial t} + c\frac{\partial}{\partial x})v = 0 \ . \tag{A.4}$$

The first term of the right hand side represent a wave moving to the left, while the second term represent a wave moving in the opposite direction. And the transport equations have the following characteristic equations

$$x + ct = const \tag{A.5}$$

$$x - ct = const$$

that recommends the following change in variables

$$\zeta = x + ct \tag{A.6}$$

$$\eta = x + ct$$

using the chain rule the partial derivatives could be expressed as follows

$$
\begin{aligned}
\frac{\partial v}{\partial x} &= \frac{\partial v}{\partial \zeta}\frac{\partial \zeta}{\partial x} + \frac{\partial v}{\partial \eta}\frac{\partial \eta}{\partial x} = \frac{\partial v}{\partial \zeta} + \frac{\partial v}{\partial \eta} \\
&= v_\zeta + v_\eta
\end{aligned} \tag{A.7}
$$

$$
\begin{aligned}
\frac{\partial v}{\partial t} &= \frac{\partial v}{\partial \zeta}\frac{\partial \zeta}{\partial t} + \frac{\partial v}{\partial \eta}\frac{\partial \eta}{\partial t} = c\,\frac{\partial v}{\partial \zeta} - c\,\frac{\partial v}{\partial \eta} \\
&= c\,v_\zeta - c\,v_\eta
\end{aligned} \tag{A.8}
$$

$$
\frac{\partial^2 v}{\partial x^2} = \frac{\partial}{\partial x}\Big(\frac{\partial v}{\partial x}\Big) = v_\zeta^2 + v_\eta^2 + 2 v_\zeta v_\eta \tag{A.9}
$$

$$
\frac{\partial^2 v}{\partial t^2} = \frac{\partial}{\partial t}\Big(\frac{\partial v}{\partial t}\Big) = c^2 v_\zeta^2 + c^2 v_\eta^2 - 2c^2 v_\zeta v_\eta \;. \tag{A.10}
$$

Since
$$
\frac{\partial^2 v(x,t)}{\partial t^2} - c^2\frac{\partial^2 v(x,t)}{\partial x^2} = 0 \;. \tag{A.11}
$$

plugging the partial derivatives and canceling the similar terms out we get

$$
-4c^2 v_\zeta v_\eta = 0 \;. \tag{A.12}
$$

That in turn implies
$$
\frac{\partial}{\partial \eta}\Big(\frac{\partial v}{\partial \zeta}\Big) = 0 \;. \tag{A.13}
$$

This indicates that $\frac{\partial v}{\partial \eta}$ is independent of η

$$
\therefore \frac{\partial v}{\partial \eta} = \Gamma(\zeta)
$$

taking the integral of both sides we get

$$
v = \int \Gamma(\zeta) + G(\eta)
$$

$$\therefore v = F(\zeta) + G(\eta) .$$

Changing the variables back, we get the solution of the homogenous part, where F is some arbitrary function, while G is some other arbitrary function that could be determined by using the initial and boundary conditions

$$v(t, x) = F(x + ct) + G(x - ct) \tag{A.14}$$

where $F(x + ct)$ is a wave moving to the left, while $G(x - ct)$ is another wave moving to the right. Both waves cancel out and add up when the interact in a linear manner. Using the initial position we get

$$v(x, 0) = f(x) \Rightarrow F(x) + G(x) = f(x) \tag{A.15}$$

and the initial velocity

$$v_t(x, 0) = g(x) \Rightarrow c\frac{dF(x)}{dt} - c\frac{dG(x)}{dt} = g(x) \tag{A.16}$$

integrating Eq.A.16 from 0 to x

$$c\left(F(x) - G(x)\right) = \int_o^x g(s)ds + c_1 \tag{A.17}$$

$$F(x) - G(x) = \frac{1}{c} \int_o^x g(s)ds + c_2 .$$

From Eq.A.15

$$F(x) + G(x) = f(x) .$$

Solving the previous two equations with each other we get

$$F(x) = \frac{1}{2}f(x) + \frac{1}{2c} \int_o^x g(s)ds + c_3 \tag{A.18}$$

$$G(x) = \frac{1}{2}f(x) - \frac{1}{2c} \int_o^x g(s)ds - c_3 \tag{A.19}$$

recalling eq.A.14

$$v(t, x) = F(x + ct) + G(x - ct)$$

$$v(t,x) = \frac{1}{2}[f(x+ct) + f(x-ct)] + \frac{1}{2c}[\int_o^{x+ct} g(s)ds - \int_o^{x-ct} g(s)ds] \ .$$

The solution of the homogenous part of the wave equation is

$$v(t,x) = \frac{1}{2}[f(x+ct) + f(x-ct)] + \frac{1}{2c}[\int_{x-ct}^{x+ct} g(s)ds] \ . \tag{A.20}$$

For the forced response we have to solve the non-homogenous wave equation

$$\frac{\partial^2 w(x,t)}{\partial t^2} - c^2\frac{\partial^2 w(x,t)}{\partial x^2} = H(t,x)$$

changing the variables into

$$\zeta = x + ct$$

$$\eta = x + ct$$

computing the partial derivatives just as the homogenous part we get

$$\frac{\partial^2 w(x,t)}{\partial t^2} - c^2\frac{\partial^2 w(x,t)}{\partial x^2} = -4c^2\frac{\partial}{\partial\zeta}(\frac{\partial w}{\partial\eta}) \tag{A.21}$$

$$\therefore -4c^2\frac{\partial}{\partial\zeta}(\frac{\partial w}{\partial\eta}) = H(t,x)$$

$$\therefore \frac{\partial}{\partial\zeta}(\frac{\partial w}{\partial\eta}) = -\frac{1}{4c^2}H(t,x) \ .$$

By double integrating the previous equation we get the forced response of the one dimensional wave equation

$$w(t,x) = \frac{1}{2c}\int_o^t \int_{x-c(\tau-t)}^{x+c(\tau+t)} H(s,\tau)dsd\tau \ . \tag{A.22}$$

Since the total response is given by the super-position principle as follow

$$u(t,x) = v(t,x) + w(t,x)$$

we conclude that the total solution of the wave equation is

$$u(t,x) = \frac{1}{2}[f(x+ct) + f(x-ct)] + R + S \tag{A.23}$$

$$R \triangleq f(x - ct)] + \frac{1}{2c}[\int_{x-ct}^{x+ct} g(s)ds]$$

$$S \triangleq \frac{1}{2c} \int_o^t \int_{x-c(\tau-t)}^{x+c(\tau+t)} H(s,\tau)ds d\tau$$

where c is the wave propagation speed, $g(s)$ is the initial velocity, $H(s,\tau)$ is the input forcing function and $f(x)$ is the initial wave configuration or initial position.

APPENDIX B

Flexible Motion Estimation

Since the reflected torque wave is defined by the following equation

$$\widehat{\tau}_{\mathbf{ref}} = \widehat{k}(\theta_m - \theta_1) + \widehat{B}(\dot{\theta}_m - \dot{\theta}_1) \tag{B.1}$$

re-arranging the terms we obtain

$$\widehat{B}\dot{\theta}_1 + \widehat{k}\theta_1 = \widehat{B}\dot{\theta}_m + \widehat{k}\theta_m - \widehat{\tau}_{\mathbf{ref}} \ . \tag{B.2}$$

Defining

$$\alpha \triangleq \widehat{B}\dot{\theta}_m + \widehat{k}\theta_m - \widehat{\tau}_{\mathbf{ref}}$$

rewriting Eq.B.2

$$\widehat{B}\dot{\theta}_1 + \widehat{k}\theta_1 = \alpha$$

$$\beta \triangleq \frac{\alpha}{\widehat{B}}$$

the standard form is

$$\dot{\theta}_1 + \frac{\widehat{k}}{\widehat{B}}\theta_1 = \beta \ .$$

Since the differential equation is based on estimated parameters and variables, the solution also will be an estimate and the equation can be rewritten as follows

$$\widehat{\dot{\theta}}_1 + \frac{\widehat{k}}{\widehat{B}}\theta_1 = \beta$$

multiplying the previous differential equation by the integrating factor $e^{\frac{\widehat{B}}{\widehat{k}}t}$

$$e^{\frac{\widehat{B}}{\widehat{k}}t}\widehat{\dot{\theta}}_1 + e^{\frac{\widehat{k}}{\widehat{B}}t}\frac{\widehat{k}}{\widehat{B}}\theta_1 = e^{\frac{\widehat{B}}{\widehat{k}}t}\beta$$

$$\frac{d}{dt}[e^{\frac{\widehat{B}}{\widehat{k}}t}\widehat{\theta}_1] = e^{\frac{\widehat{B}}{\widehat{k}}t}\beta$$

integrating both sides

$$e^{\frac{\widehat{B}}{k}t}\widehat{\theta}_1 = \int_o^t \beta e^{\frac{\widehat{B}}{k}\tau}d\tau + c \ .$$

The estimated position of the first lumped inertial mass is

$$\widehat{\theta}_1(t) = e^{-\frac{\widehat{B}}{k}t}\int_o^t \beta e^{\frac{\widehat{B}}{k}\tau}d\tau + e^{-\frac{\widehat{B}}{k}t}c_1 \ . \tag{B.3}$$

For the estimate of the second inertial mass, we recall the first equation of motion, and replacing the real parameters and variables by the estimated ones we obtain

$$J_1\ddot{\widehat{\theta}}_1 - \widehat{B}(\dot{\theta}_o - \dot{\widehat{\theta}}_1) - \widehat{k}(\theta_o - \widehat{\theta}_1) + \widehat{B}(\dot{\widehat{\theta}}_1 - \dot{\widehat{\theta}}_2) + \widehat{k}(\widehat{\theta}_1 - \theta_2) = 0 \tag{B.4}$$

defining

$$\gamma \triangleq J_1\ddot{\widehat{\theta}}_1 - \widehat{B}(\dot{\theta}_o - \dot{\widehat{\theta}}_1) - \widehat{k}(\theta_o - \theta_1) + \widehat{B}\ \dot{\widehat{\theta}}_1 + \widehat{k}\ \widehat{\theta}_1$$

rewriting eq.B.4

$$\widehat{B}\ \dot{\widehat{\theta}}_2 + \widehat{k}\ \theta_2 = \gamma$$

$$\zeta \triangleq \frac{\gamma}{\widehat{B}} \ .$$

The standard for of the 1st order differential equation is

$$\dot{\widehat{\theta}}_2 + \frac{\widehat{k}}{\widehat{B}}\ \theta_2 = \zeta \tag{B.5}$$

multiplying by the integrating factor $e^{\frac{\widehat{B}}{k}t}$

$$e^{\frac{\widehat{B}}{k}t}\dot{\widehat{\theta}}_2 + e^{\frac{\widehat{B}}{k}t}\frac{\widehat{k}}{\widehat{B}}\ \theta_2 = e^{\frac{\widehat{B}}{k}t}\zeta$$

$$\frac{d}{dt}[e^{\frac{\widehat{B}}{k}t}\ \widehat{\theta}_2] = e^{\frac{\widehat{B}}{k}t}\zeta \ .$$

Integrating both sides

$$e^{\frac{\widehat{B}}{k}t}\widehat{\theta}_1 = \int_o^t \zeta e^{\frac{\widehat{B}}{k}\tau}d\tau + c_2 \ .$$

The obtain estimate of the second inertial mass position

$$\widehat{\theta}_2(t) = e^{-\frac{\widehat{B}}{k}t}\int_o^t \zeta e^{\frac{\widehat{B}}{k}\tau}d\tau + e^{-\frac{\widehat{B}}{k}t}c_2 \ . \tag{B.6}$$

Repeating the previous procedure on the second equation of motion we get the estimate of the third mass position

$$\widehat{\theta}_3(t) = e^{-\frac{\widehat{k}}{\widehat{B}}t} \int_o^t \varepsilon \; e^{\frac{\widehat{k}}{\widehat{B}}\tau} d\tau + e^{-\frac{\widehat{B}}{\widehat{k}}t} c_3 \tag{B.7}$$

$$\varepsilon \triangleq \frac{\delta}{\widehat{B}}$$

$$\delta \triangleq J_2 \, \widehat{\ddot{\theta}}_2 - \widehat{B}(\widehat{\dot{\theta}}_1 - \widehat{\dot{\theta}}_2) - \widehat{k}(\widehat{\theta}_1 - \widehat{\theta}_2) + \widehat{B} \, \widehat{\dot{\theta}}_2 + \widehat{k} \, \widehat{\theta}_2 \;.$$

For the forth lumped mass

$$\widehat{\theta}_4(t) = e^{-\frac{\widehat{k}}{\widehat{B}}t} \int_o^t \varphi \; e^{\frac{\widehat{k}}{\widehat{B}}\tau} d\tau + e^{-\frac{\widehat{B}}{\widehat{k}}t} c_4 \tag{B.8}$$

$$\varphi \triangleq \frac{\phi}{\widehat{B}}$$

$$\phi \triangleq J_3 \, \widehat{\ddot{\theta}}_3 - \widehat{B}(\widehat{\dot{\theta}}_2 - \widehat{\dot{\theta}}_3) - \widehat{k}(\widehat{\theta}_2 - \widehat{\theta}_3) + \widehat{B} \, \widehat{\dot{\theta}}_3 + \widehat{k} \, \widehat{\theta}_3 \;.$$

The general flexible motion estimation equations are

$$\widehat{\theta}_i(t) = e^{-\frac{\widehat{k}}{\widehat{B}}t} \int_o^t \Omega \; e^{\frac{\widehat{k}}{\widehat{B}}\tau} d\tau + e^{-\frac{\widehat{B}}{\widehat{k}}t} c_i \tag{B.9}$$

where

$$\Omega \triangleq \frac{\Psi}{\widehat{B}}$$

$$\Psi \triangleq g(J_{i-1}, \widehat{\theta}_{i-1}, \widehat{\dot{\theta}}_{i-1}, \widehat{\ddot{\theta}}_{i-1}, \widehat{k}, \widehat{B})$$

where $\widehat{B}$ is the estimate of the damping coefficient, $\widehat{k}$ is the estimate of the joint stiffness, $\widehat{\theta}_{i-1}$, $\widehat{\dot{\theta}}_{i-1}$ and $\widehat{\ddot{\theta}}_{i-1}$ are the position, velocity and acceleration estimates of the $i - 1^{th}$ mass and c_i is the integration constant.